Available online at www.sciencedirect.com
SCIENCE DIRECT®
Coordination Chemistry Reviews 249 (2005) 2591–2611
COORDINATION CHEMISTRY REVIEWS
www.elsevier.com/locate/ccr

Review

Magnetism of metal-nitroxide compounds involving bis-chelating imidazole and benzimidazole substituted nitronyl nitroxide free radicals

Dominique Luneau [a,b,*], Paul Rey [b]

[a] *Université Claude Bernard Lyon-1, Laboratoire des Multimatériaux et Interfaces (UMR 5615), Campus de La Doua, 69622 Villeurbanne Cedex, France*
[b] *CEA-Grenoble, Service de Chimie Inorganique et Biologique, DRFMC, 17 rue des Martyrs 38054 Grenoble Cedex 09, France*

Received 8 November 2004; accepted 22 June 2005
Available online 27 July 2005

Contents

Abstract

Coordination compounds based on imidazole and benzimidazole substituted nitronyl nitroxide radicals with transition metal ions and trivalent lanthanide ions are described from the perspective of their magnetic properties.

For the transition metal compounds the crystal structures show various metal-nitroxide dimensionalities including mononuclear (0D), one-dimensional (1D) and two-dimensional (2D) complexes. The mononuclear complexes were isolated with most metal ions of the first transition series. One copper(II) complex shows a copper(II)–radical ferromagnetic coupling ($J = +75\ cm^{-1}$) while for the other mononuclear compounds, mainly with manganese(II), the metal–radical interactions are antiferromagnetic. The one-dimensional and two-dimensional complexes are manganese(II) compounds which show canting effects leading to weak ferromagnetism.

For the trivalent lanthanide ions [La(III), Gd(III) and Eu(III)], three series of mononuclear complexes were obtained in which the metal center is bound to four, two or one nitroxide radicals depending on the counter ions and ancillary ligands. Unexpectedly, in most gadolinium(III) complexes, the Gd(III)–radical interactions were found to be antiferromagnetic in contradiction with other foundings and previous theoretical models. In support to the magnetic studies, the optical properties of the lantanide complexes have also been investigated and are briefly described.

Keywords: Nitronyl nitroxide; Complex; Copper(II); Manganese(II); Nickel(II); Zinc(II); Gadolinium(III); Europium(III); Lanthanum(III); Magnetism; Luminescence; Absorption

* Corresponding author. Tel.: +33 4 72 43 14 18; fax: +33 4 72 43 11 60.
E-mail address: luneau@univ-lyon1.fr (D. Luneau).

0010-8545/$ – see front matter © 2005 Elsevier B.V. All rights reserved.
doi:10.1016/j.ccr.2005.06.008

1. Introduction

From the general point of view, the strategy to get magnetic materials by coordination chemistry, relies on building extended polymetallic networks in which magnetic metal centres are connected through bridging ligands. The latters should both assemble the metal centres and mediate strong magnetic interactions, and in such a way to have a bulk non-zero magnetic moment. In this context, the use of free radicals as the bridging ligands is particularly pertinent. First, the direct bonding of the spin carriers, that is the metal centers and the free radical, should favour strong magnetic interactions. Second, the combination of inorganic and organic spin carriers allows a great versatility in the design of magnetic networks with various topologies and dimensionalities.

Whereas the metal–radical approach should not be restricted to the only nitroxide free radicals, the latter ones have gained predominance and dragged much works in the last two decades. This should be ascribed to the fact that nitroxide radicals are among the most persistent free radicals even in the presence of metal ions and may be obtained in almost limitless forms thus allowing the fine design of a large panel of magnetic bridging ligand.

The scope of the present review with respect to magnetic materials is not to cover all the results involving nitroxide–metal complexes for which some reviews have already appeared [1–5]. It concerns mostly the complexes of nitronyl or imino nitroxide grafted on imidazolyl or benzimidazolyl groups (Scheme 1) and is mainly based on our published work supported by some unpublished results.

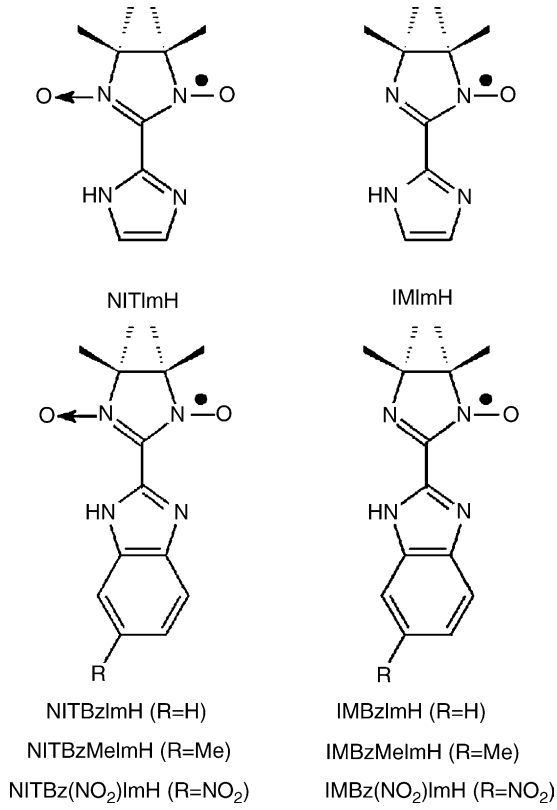

Scheme 1.

2. Background

Nitroxide free radicals are one of the best characterized groups of free radicals. Their prior interest was mainly as probes in biological systems and most of the early studies on metal-nitroxide interactions were related to this field [6]. It is in the last two decades that they became increasingly appealing as spin carriers in magnetic materials. Thus, the first organic magnets were nitroxide free radicals [7,8] and their discovery in the 1990s gave rise to extending research works dedicated to purely organic molecular based magnets [9,10].

However, the first mention of nitroxide free radical relevant to molecule-based magnetic materials was reported in the 1970s by Lim and Drago and concerned a complex in which 2,2,6,6-tetramethylpipridinyl-1-oxy free radical (TEMPO) was coordinated by the NO group [11]. This work really set up the basis of nitroxide coordination chemistry. Indeed, the main drawback of nitroxide radicals has long been the poor ability of the N–O nitroxyl group to coordinate, but in their paper Lim and Drago [11] demonstrated that it could well coordinate if a strong acidic metal centres, such as bis(hexafluoroacetylacetonato)copper(II) was used. This result was then confirmed by several other reports [12–18] which concerned complexes of copper(II) and manganese(II) acetylacetonato (hfac) or trihaloacetato ($O_2CC\ X_3$) mostly with 2,2,6,6-tetramethylpipridinyl-1-oxy (TEMPO) or 2,2,5,5-tetramethylpyrrolidinyl-1-oxy (PROXYL) [13–18] (Scheme 2) and in one case it concerned a nitronyl nitroxide radical [12]. These pioneering works were also of great relevance from the magnetic point of view as they generally demonstrated the presence of strong metal-nitroxide magnetic interactions in these systems [12,13,15,17–20].

It was Gatteschi and Rey [1,2] who first used metal-nitroxide complexes in the engineering of molecule-based magnets. Their approach was to use nitronyl nitroxide radicals as bridging ligands (Scheme 3).

Indeed, nitronyl nitroxides have two symmetrically NO groups available for coordination. Moreover, as demonstrated

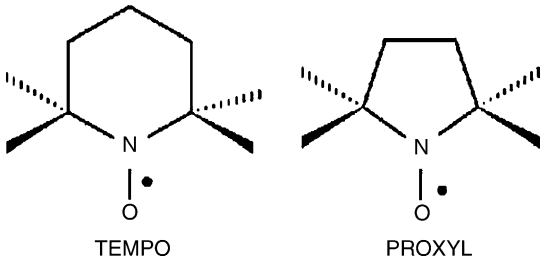

Scheme 2.

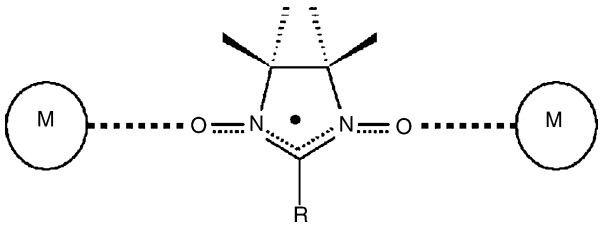

Scheme 3.

by theoretical calculations and polarized neutron studies, the unpaired electron is equally delocalised on both NO groups [21,22]. Following their approach, they succeeded in synthesizing one-dimensional (1D) metal-nitroxide compounds with magnet like behaviour [23–26]. These results demonstrated that nitroxide coordination was efficient for the rational design of molecular based materials and they really initiated this field. We refer the reader to reviews covering these pioneering works [1,2].

However, because of the one-dimensional character of the metal-nitroxide network of these compounds, bulk magnetization was observed only at low temperature (<20 K). It soon became evident that any increase of the Curie temperature had to deal with increasing the dimensionality of the metal-nitroxide network. In order to do so one way has been to add extra coordination sites on the nitronyl nitroxide [27–29] or to use polynitroxide radicals [3,30–32]. An other alternative in which we have been very active and which form the basis of the present article has been to increase the number of radicals around each metal ion. This requires to get rid of the bulky and electro-withdrawing ancillary ligands, such as the hfac. Thus, using 2-(2-pyridyl)-substituted nitronyl nitroxide free radicals (NITPy), we first demonstrated with metal chlorides complexes that this could be achieved if the N–O group of the nitronyl nitroxide was incorporated in a chelate ring in order to force the metal coordination [33]. Since then, numerous metal complexes of transition metal and lanthanide ions have been reported with chelating nitronyl or imino nitroxide radicals grafted on various groups, such

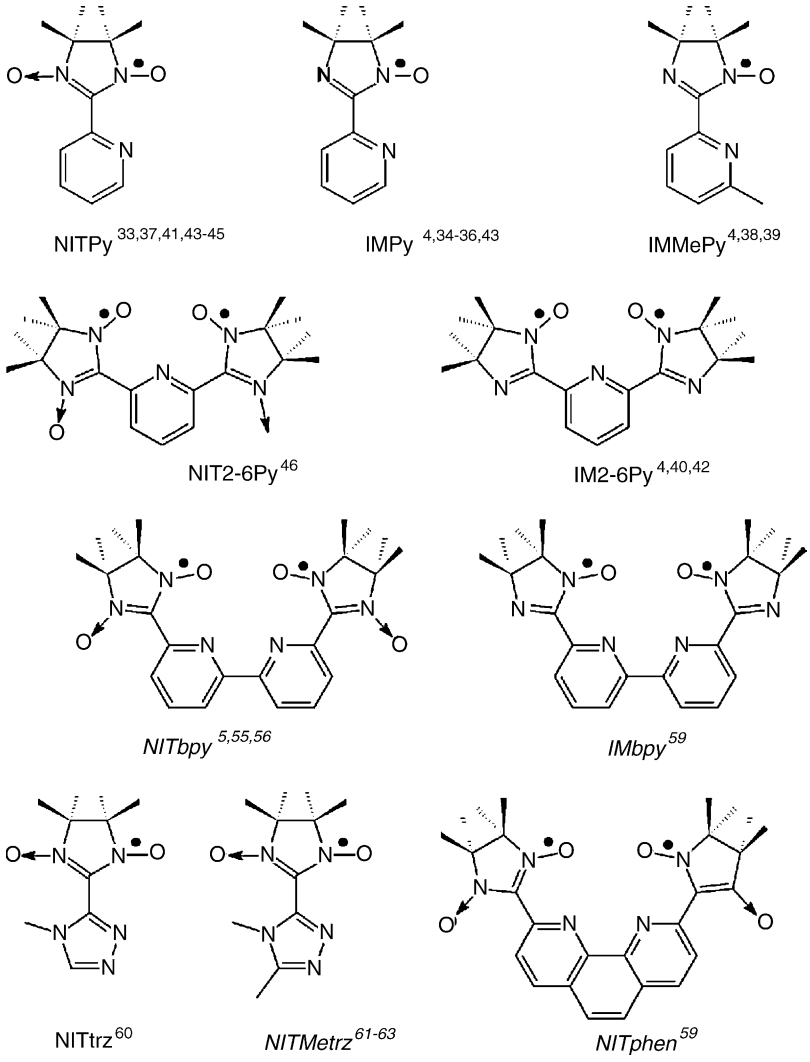

Scheme 4.

as pyridine [4,33–46], imidazole [41,47–50], benzimidazole [41,43,49,51–54], bipyridine [5,55–58], phenanthroline [59] or triazole [60–63] (Scheme 4). These complexes exhibit different topologies and dimensionality including molecular species (0D) [4,33–43,46,51,53,54], one-dimensional compounds [47], two-dimensional compounds (2D) [48,49,52] and also clusters [44,45].

3. Scope of the review

The present article is mainly a review of our cumulative work with nitronyl and imino-nitroxide grafted on to imidazole or benzimidazole groups (Scheme 1). These ligands have also been studied by others but mainly as organic building blocks [64–67]. In our case, these radicals were specially designed in order to have, after deprotonation of the imidazolyl amino group, two symmetrical chelating sites incorporating the NO groups (Scheme 5).

We had in mind that the resulting bis-chelating nitronyl nitroxide radicals would behave in a way reminiscent of oxalato and oxamato ligands which have proved to be efficient for the design of 2D and 3D polymetallic networks with interesting magnetic properties [68–70]. Our idea was to use the deprotonated imidazole or benzimidazole substituted nitronyl nitroxides instead of the diamagnetic ligands with the expectation to get related structures exhibiting bulk magnetization with high T_c temperatures (Scheme 6).

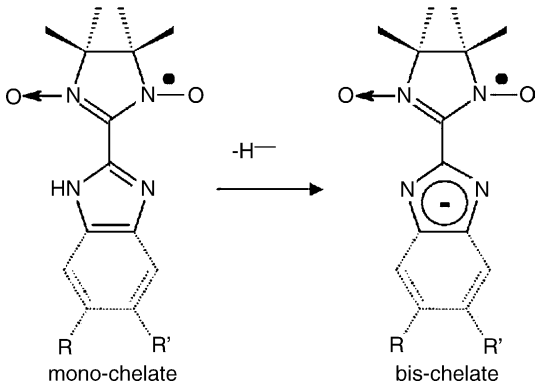

Scheme 5.

Over the last few years, our quest for such magnetic compounds led us to synthesize and study numerous complexes of these nitronyl and imino nitroxide radicals (Scheme 1) both with transition metal ions and lanthanides. A crystal structure has been established for most of them showing various metal-nitroxide dimensionalities including molecular precursors, one-dimensional and two-dimensional complexes. Their magnetic properties range from the isolated multi-spin systems to compounds exhibiting spontaneous magnetization. The studies of the lanthanide complexes led us also to extend the optical properties of both metal–radical complexes and of the free radicals in relation to their magnetic properties. It is these results which form the basis of this review.

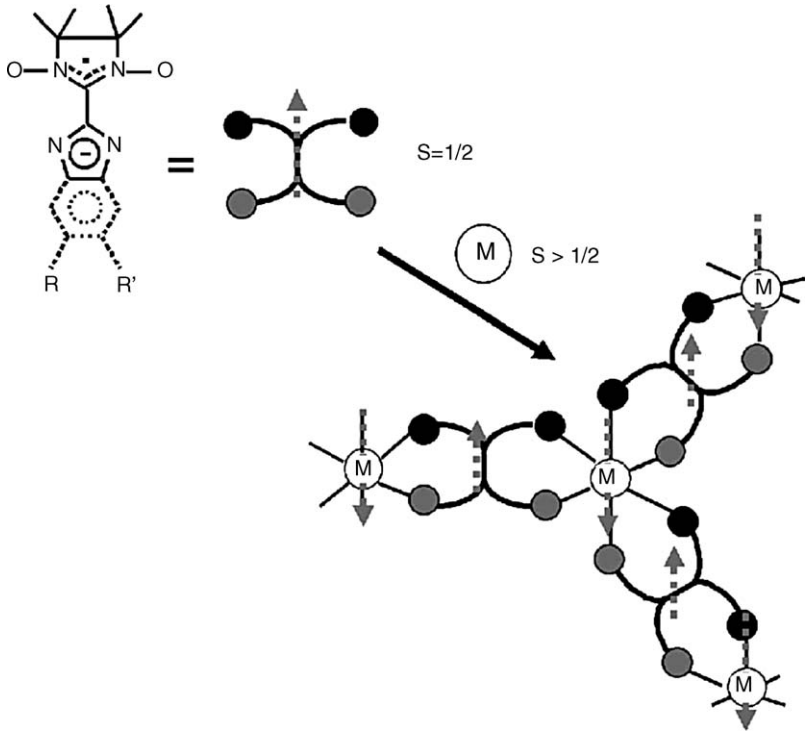

Scheme 6.

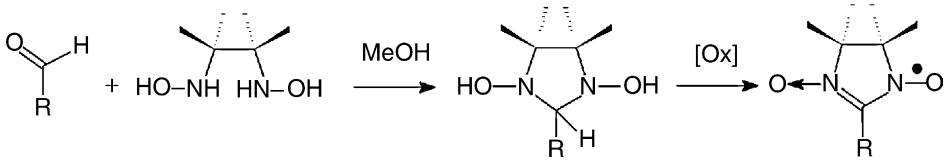

Scheme 7.

3.1. Synthesis

3.1.1. Synthesis of the radicals

All nitronyl nitroxide radicals reported here were synthesized following Ullman's two steps procedure (Scheme 5) [71,72]. First, a precursor aldehyde is condensed with 2,3-bis(hydroxyamino)-2,3-dimethylbutane [73] in methanol. The resulting bis-hydroxyimidazolidine is then converted to the nitronyl nitroxide radical by oxidation using $NaIO_4$ using in a two-phase mixture H_2O/CH_2Cl_2 (Scheme 7).

According to this procedure, any modification of the nitronyl nitroxide occurs by way of an appropriate aldehyde. In the present case, NITImH and NITPy were synthesized, respectively, from commercial 2-imidazolcarboxaldehyde and 2-pyridinecarboxaldehyde. In the case of NITBzIMH and its substituted derivatives, the aldehydes were synthesized as previously reported for 2-benzimidazolcarboxaldehyde [47]. Note that a new procedure was recently found allowing modification of the imidazoline ring in four and five positions [73].

The imino nitroxide radicals were obtained from the corresponding nitronyl nitroxides by dissolving in an aqueous solution of sodium nitrite and further treatment with dilute hydrochloric acid (Scheme 8) [50,74].

3.1.2. Synthesis of the complexes

All mononuclear compounds of transition metal ions were obtained in the form of single crystals by mixing stoichiometric amounts of the reactants in methanol or ethanol followed by slow evaporation of the resulting solution in the dark at room temperature [41]. In the case of the lanthanides, the perchlorates compounds were obtained from THF, the nitrate in ethanol and the hfac derivatives in mixture of heptane and chloroform [43,54]. Single crystals of the one-dimensional and two-dimensional compounds were obtained by slow diffusion of the reactants [47,48].

Safety notes: Metal perchlorates containing organic ligands are potentially explosive. Only a small amount of material should be prepared, and it should be handled with great care.

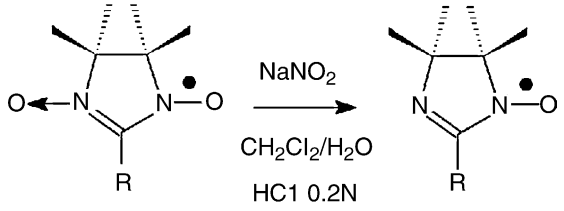

Scheme 8.

3.2. Transition metal compounds

3.2.1. Mononuclear complexes

This part concerns the compounds for which the imidazole ring has not been deprotonated. In that case the nitronyl nitroxides behave as mono-chelating ligands and are not bridging. The resulting complexes may be viewed as the molecular building blocks for further extended complexes.

There were good reasons to be interested in the mononuclear complexes. First, it was important in view to build extended metal–radical networks to test the chelating effect to any metal ions and moreover to know how many radicals can fit around each metal centre. For these reasons, the synthesis was mainly focussed at complexes with the weakly coordinating perchlorate anions. Second, the mononuclear complexes, as simple spin systems, are essential for the study of the metal–radical magnetic interactions in such compounds and for further understanding of the magneto-structural relation in extended compounds.

3.2.2. Copper(II) compounds

As may be foreseen, the reaction of copper(II) perchlorate with NITImH led to $[Cu(NITImH)_2(ClO_4)_2]$ (**1**) in which copper(II) ion accommodates only two NITImH radicals in a chelating mode (Fig. 1). The coordination sphere is an

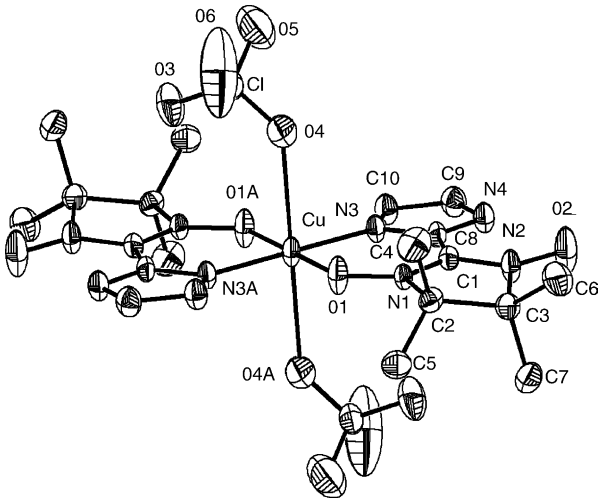

Fig. 1. Molecular structure of complex $[Cu(NITImH)_2(ClO_4)_2]$ **1**.

Table 1
Selected bond length (Å) in compounds **1**–**7**

	M–O1A	M–O1B	M–O1C	M–N3A	M–N3B	M–N3C
1	1.955(4)			1.953(4)		
2	2.181(3)	2.199(4)	2.142(4)	2.206(4)	2.257(4)	2.214(4)
3	2.180(4)	2.134(3)	2.175(3)	2.209(4)	2.175(3)	2.227(4)
4	2.121(6)	2.058(7)	2.122(6)	2.060(7)	2.110(7)	2.090(7)
5	2.122(6)	2.064(7)	2.132(6)	2.088(7)	2.109(7)	2.068(7)
6	2.109(6)	2.049(7)	2.120(6)	2.074(8)	2.069(8)	2.052(8)
7	2.17(1)	2.12(1)	2.17(1)	2.07(1)	2.08(1)	2.11(1)

elongated octahedron with the two radicals in the equatorial plane [Cu–O1 1.955(4) Å and Cu–N3 1.953(4) Å] and the two perchlorate ions in trans and axial configuration [Cu–O4 2.532(4) Å] (Table 1).

The magnetic studies revealed that the copper(II) ion is ferromagnetically coupled with both nitroxide radicals. At 300 K the χT value is 1.30 emu K mol^{-1} and reaches a maximum of 1.71 emu K mol^{-1} at 40 K correlating well with the value for a ground spin state $S_t = 3/2$ corresponding to three $S = 1/2$ spins which are ferromagnetically coupled (Fig. 2). The ground spin state $S_t = 3/2$ was also confirmed by magnetization measurement. The simulation of the experimental data with a linear symmetrical model of three spin $S = 1/2$ gave a good fit with one magnetic Cu(II)–radical coupling constant $J = +75$ cm^{-1} and $g_{rad} = g_{Cu} = 2.1$ [$H = -2J(S_1S_2 + S_1S_3]$].

This is a rare example where equatorial coordination copper-nitroxide gives a ferromagnetic coupling. Indeed, in most copper(II)-nitroxide complexes involving hexafluoracetylacetonato (hfac) and in which the nitroxide radicals are bound only by the nitroxyl oxygen atoms the equatorial coordination leads to strong antiferromagnetic interactions while the axial coordination favours ferromagnetic interactions [2]. In the present case, the chelate results in a low value of the angle between the M–O–N plane and the imidazoline plane which are almost coplanar (Table 1). This geometry has the effect to bring the SOMO π^* magnetic orbital of both radicals orthogonal with the dx^2-y^2 magnetic orbital of the copper(II) ion, which results, as is known, in ferromagnetic interaction [75]. Moreover, the large value ($J = +75$ cm^{-1}) of the ferromagnetic interaction should be ascribed to the fact that the Cu–ON bond distance are quite short in this compound (Table 1).

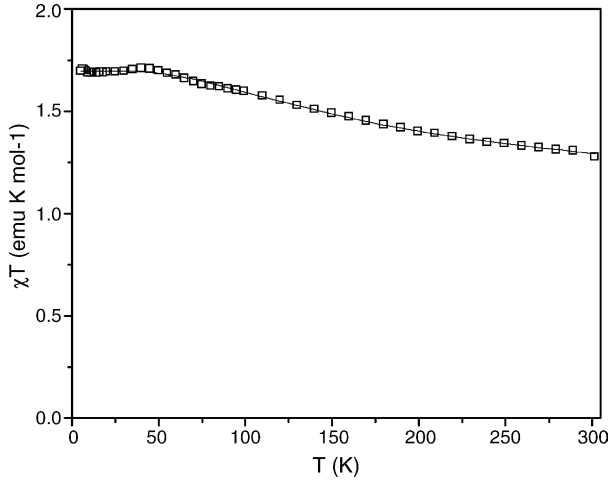

Fig. 2. Temperature dependence of χT for compound [Cu(NITImH)$_2$(ClO$_4$)$_2$] (**1**). The solid lines represents the best fit to the data with values reported in the text.

3.2.3. Manganese(II), cobalt(II), nickel(II), zinc(II) compounds [41]

NITImH and NITBzImH react with the perchlorate salts of Mn(II), Co(II), Ni(II), Zn(II) to form compounds [M^{II}(NITImH)$_3$](ClO$_4$)$_2$ [M = Mn (**3**, **4**), Co (**5**), Ni (**6**), Zn (**7**)] and [Mn^{II}(NITBzImH)$_3$](ClO$_4$)$_2$ (**2**) in which each metal centre is fully coordinated by three chelating radicals. Similar compounds [M^{II}(NITPy)$_3$](ClO$_4$)$_2$ [M = Mn, Co, Ni] were also obtained with 2-(2-pirydyl) substituted nitronyl nitroxide NITPy. This demonstrates, if needed, how the strategy of using chelating nitroxide is efficient to coordinate weakly acidic metal centres. In compounds **2**–**7** as expected from the M(X–Y)$_3$ coordination pattern both *fac* (OC-6-21) and *mer* (OC-6-22) stereoisomeric geometries of the [M(radical)$_3$]$^{2+}$ complex were observed in addition to their Λ and Δ enantiomeric forms. The *fac* geometry was observed for compounds **3** and **7** while the *mer* form was found for compounds **2** and **4**–**6**. It is only in the case of the Mn(II) complexes with NITImH that both *fac* (**2**) and *mer* (**3**) were obtained. In fact, compound **4** was obtained as a low yield side-product in the synthesis of a two-dimensional compound. The different *fac* and *mer* stereoisomers are exemplified with those of the Mn(II) complexes in Figs. 3 and 4.

In all compounds **2**–**7**, the metal–ligand bond distances are within the expected range (Table 1) for the respective metal ions but as expected, the coordination sphere is a distorted octahedron. In all complexes, the three nitroxide free radicals show the expected elongation (≈0.1 Å) of the N–O bond of the coordinated oxyl groups [2].

The *mer* and *fac* stereoselectivity observed for the complexes in these compounds was ascribed to the balance between minimisation of the steric crowding around the metal ion and maximization of the crystal packing. The *fac* steroisomers being more symmetrical (C3 symmetry) than the *mer* isomers tend to maximise the crystal packing as is observed from density (Table 2) but the *fac* geometry induces higher steric crowding compared with the *mer* isomers. This is the reason why the *fac* isomers are observed with the smaller radi-

Table 2
Calculated density for compounds **2**–**4**

	Compounds	Isomer	d (g cm^{-3})
2	[Mn^{II}(NITBzImH)$_3$](ClO$_4$)$_2$	*mer*	1.421
3	[Mn^{II}(NITImH)$_3$](ClO$_4$)$_2$	*fac*	1.503
4	[Mn^{II}(NITImH)$_3$](ClO$_4$)$_2$	*mer*	1.355
5	[Co^{II}(NITImH)$_3$](ClO$_4$)$_2$	*mer*	1.358
6	[Ni^{II}(NITImH)$_3$](ClO$_4$)$_2$	*mer*	1.386
7	[Zn^{II}(NITImH)$_3$](ClO$_4$)$_2$	*fac*	1.524

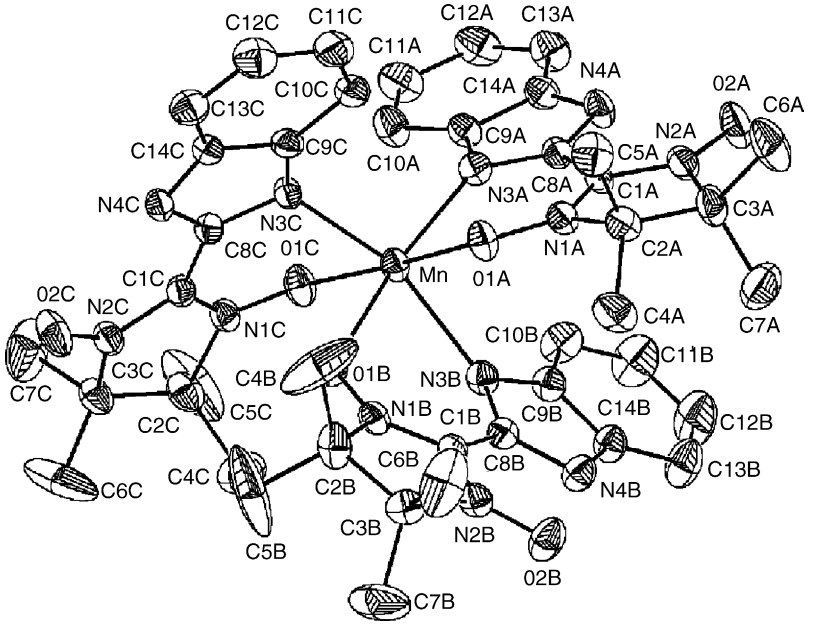

Fig. 3. Molecular structure of complex *mer*-$[Mn^{II}(NITBzImH)_3]^{2+}$ (**2**). Reproduced with permission from Ref. [41].

cal NITImH and with the Mn(II) (**3**) and Zn(II) (**7**) which have as usually the most expanded coordination sphere of the first transition metal(II) series, while the *mer* forms are favoured for Co(II) (**5**) and Ni(II) (**6**) which have a less expanded coordination sphere. In the case of the NITBzImH ligand, the *mer* form is always favoured (**2**), even with Mn(II), because the NITBzImH ligand is much bulkier.

Regarding the magnetic properties, the *fac* and *mer* forms should be considered differently. In the *fac* compounds (**3**, **7**), relatively short intramolecular distances (2.95 Å) between the coordinated N–O groups within the coordination sphere are observed which may be considered as relevant for magnetism. Moreover, compounds **3** and **7** are isomorphous and the complexes $[M^{II}(NITImH)_3]^{2+}$ make dimers by staking of two imidazole fragments with short spacing of 3.24(5) Å. In the *mer* compounds (**2**, **4**–**6**), as mentioned above, the crystal packings are less compact and much larger intermolecular distances are observed so that the $[Mn^{II}(radical)_3]^{2+}$ complexes may be considered as isolated four spin systems from the magnetic point of view.

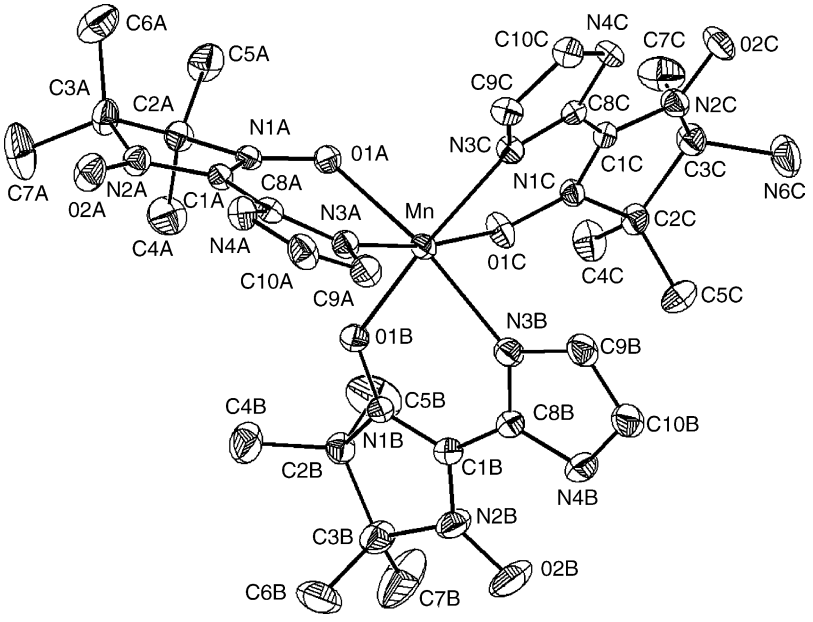

Fig. 4. Molecular structure of complex *fac*-$[Mn^{II}(NITImH)_3]^{2+}$ (**3**). Reproduced with permission from Ref. [41].

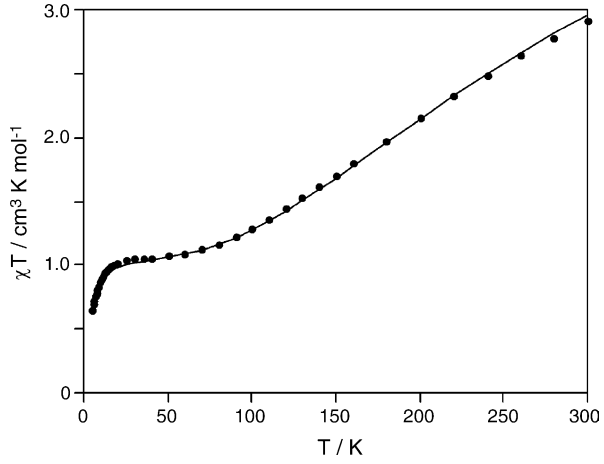

Fig. 5. Temperature dependence of χT for compound $[Mn^{II}(NITImH)_3](ClO_4)_2$ (**3**). The solid line represents the best fit of the data with values reported in the text. Reproduced with permission from Ref. [41].

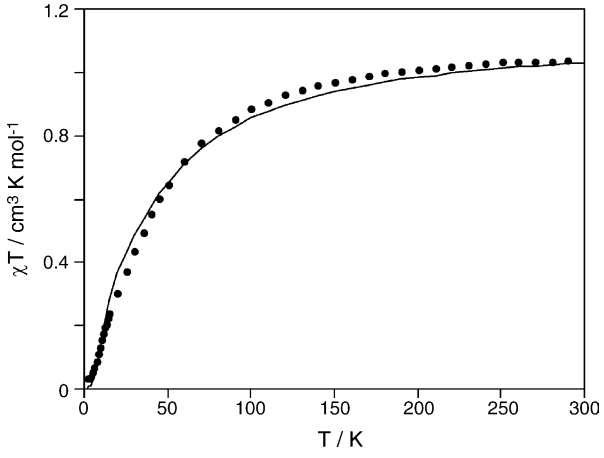

Fig. 6. Temperature dependence of χT (●) for compound $[Zn^{II}(NITImH)_3](ClO_4)_2$ (**7**). The solid line represents the best fit of the data with values reported in the text. Reproduced with permission from Ref. [41].

An overall antiferromagnetic behaviour is observed for all compounds **2**–**7**.

The two manganese(II) compounds $[Mn^{II}(NITBzImH)_3](ClO_4)_2$ (**2**) and $[Mn^{II}(NITImH)_3](ClO_4)_2$ (**3**) (Fig. 5) show the same thermal behaviour. At 300 K, the χT value [$\chi T = 2.9$ (**2**) and 2.5 (**3**) emu K mol^{-1}] is much weaker than expected for four independent spins. Then on cooling it decreases to reach a plateau whose value ($\chi T \approx 1$ emu K mol^{-1}) corresponds well to a ground spin state $S_t = 1$ as expected for one Mn(II) ($S = 5/2$) antiferromagnetically coupled with three radicals ($S = 1/2$). The ground spin state $S_t = 1$ was also confirmed by magnetization saturation experiments. The fitting of the experimental magnetic susceptibility gave metal-nitroxide couplings: (**2**) $J = -79(5)$ cm^{-1} and (**3**) $J = -53(2)$ cm^{-1} ($H = -2J\Sigma S_i S_j$) and weak intermolecular interactions (**2**) $zJ' = -0.7(3)$ cm^{-1} and (**3**) $zJ' = -1.4(3)$ cm^{-1} Compound **4** was obtained in a too small quantity to allow the study of its magnetic behaviour.

Overall antiferromagnetic behaviour was also observed for the nickel(II) (**6**) and cobalt(II) (**5**) compounds. For **5**, at 300 K the χT value (2.65 emu K mol^{-1}) is weaker than expected for the independent spins and, on cooling, decreases continuously to approach zero at 2 K. No attempts have been made to determine the coupling constant. For **6** at 300 K the χT value (2.12 emu K mol^{-1}) is close to that expected for the independent spins and on cooling it decreases continuously to approach unity at 2 K. However, the χT value below 50 K depends on the rate of cooling and measurements were not reproducible indicating that the compound may be subject to crystallographic modifications inducing changes within the coordination sphere and therefore of the coupling interactions. Thus, the simulation of the magnetic susceptibility was carried only between 50 and 300 K. This gave a good fit with three different Ni(II)–radical coupling constants, one ferromagnetic ($J_1 = 13$ cm^{-1}) and two antiferromagnetic ($J_2 = -7$ cm^{-1} and $J_3 = -50$ cm^{-1}) and $g = 2.11$.

The zinc(II) compound (**7**) was intended to provide an estimate of the magnitude of the coupling between the radicals within the coordination sphere. However, the magnetic study revealed a more complex behaviour. Indeed, for compound (**7**) χT decreases continuously on cooling and approaches zero as the temperature reaches 2 K (Fig. 6). This cannot be explained by taking in account only the antiferromagnetic coupling of the radicals within the complex $[Zn^{II}(NITImH)_3]^{2+}$ for in that case a ground doublet spin state was expected, in contrast to what is observed. In fact, as mentioned above, the molecules are arranged in dimers in the cystal. This leads to a four-spin system in which the interaction between the nitroxide radicals within the coordination sphere is not the dominant one. Thus, the magnetic data were well fitted to a model taking in account the radical–radical interaction ($J_{rad-rad} = -14$ cm^{-1}) within the complex $[Zn^{II}(NITImH)_3]^{2+}$ and the dimeric nature of the structure ($J_{dimer} = -24$ cm^{-1}). This is in contrast with the manganese(II) analogue **3** which is isomorphic with **7** but for which the magnetic behaviour was perfectly fitted without the help of intramolecular radical–radical interactions. Moreover, the intermolecular interaction zJ' was found antiferromagnetic and weaker than 1.5 cm^{-1}. This stems from the fact that, at low temperature, the triplet ground spin state is almost not affected by the radical spin carriers because the manganese-nitroxide interaction is dominant by one order of magnitude. Simple calculations show that the contribution of each nitroxide ligand to the magnetic moment of the ground spin state is only −1/4 while that of the manganese ion is +7/4. Therefore, except for **7** in which the metal ion is diamagnetic, in all other compounds the magnitude of the antiferromagnetic metal–radical coupling minimizes the role of the radical–radical coupling.

For the two manganese(II) compounds (**2**–**3**), the coupling constants compare well with those observed in complexes of the chelating nitronyl nitroxide NITPy with manganese chloride [−79(5) cm^{-1}] [33] and manganese perchlo-

Table 3
Structural parameters relevant to magnetic properties in compounds **1–6**

	M–O–N (°)			β[a] (°)		
	A	B	C	A	B	C
1	125.5(2)			6.7(2)		
2	125.1(3)	122.6(3)	117.3(3)	23.9(2)	35.6(3)	40.6(3)
3	125.4(3)	128.1(3)	129.1(3)	9.6(2)	31.3(4)	18.9(4)
4	124.3(2)	125.2(3)	126.41(3)	24.4(2)	24.0(2)	19.5(2)
5	123.9(4)	124.6(4)	126.3(4)	24.1(3)	23.2(3)	17.1(3)
6	124.0(5)	124.4(6)	126.1(5)	24.1(3)	24.3(4)	11.9(4)

Letters A, B and C hold for the three different radicals within the coordination sphere.
[a] Angle between the M–O–N plane and the imidazoline plane.

rate ($-88(5)\,cm^{-1}$) [41]. In contrast, these values are much weaker than those ($2J < -200\,cm^{-1}$) observed in complexes involving hexafluoracetylacetonato (hfac) and in which the nitroxide radicals are bound only by the nitroxyl oxygen atoms without any chelating effect [26]. This suggests that binding of the imidazole in a chelating mode lessens the magnitude of the exchange coupling. Indeed, formation of the chelate ring results in low values of the angles between the M–O–N plane and the imidazoline plane (Table 3). If one considers that the antiferromagnetic interaction results primarily from overlap of the SOMO nitroxide-magnetic orbital with the metal orbital pointing toward this ligand [75] this should result in a large weakening of the overlap and thus of the exchange value. This is for the same reason that the copper(II) complex (**1**) exhibits a strong Cu–radical ferromagnetic interaction (vide infra). Also, in contrast to complexes in which the nitroxide radicals are bound only by the nitroxyl oxygen atoms, the value of the M–O–N angle varies little in all compounds (**1**–**7**) (Table 3). Indeed, this feature is almost fixed by the chelate ring and has almost no effect on the overlap. Another reason may be that the binding is weaker compared to the hfac adducts and thus the exchange coupling is expected to decrease.

3.2.4. One-dimensional complexes [48]

The mononuclear complexes **2**–**7** described above illustrate the role of the chelating nitroxides to obtain metal-nitroxide complexes without any help of electron-withdrawing ligands. These mononuclear complexes, $[M^{II}(NITImH)_3]^{2+}$, may be regarded as molecular building blocks for further extended systems after deprotonation of the imidazolyl amino group (Scheme 3). In that context, the manganese(II) complexes are particularly interesting. Indeed, manganese(II) is spin $S = 5/2$ and in compounds (**2**, **3**) the Mn–radical interaction is antiferromagnetic. Therefore, they are good candidates for building extended compounds in which antiferromagnetically coupled alternating spins ($S = 5/2$ and 1/2) would result in ferrimagnetic behaviour.

As for most compounds containing imidazolyl groups, the main difficulty to synthesize extended compounds was to avoid precipitation upon deprotonation. Strong bases, such as NaOMe, NaOH gave insoluble and amorphous mixtures. Thus, all syntheses aimed at preparing extended manganese–radical networks were conducted using "soft" deprotonating agents, such as pyridine, imidazole, or manganese-acetate. Extended compounds were obtained with the three bases but the latter was found the most versatile as a base and metal provider but also because it gave the possibility to vary the counter anions.

Depending on the base and on the counter anions different compounds were obtained including one-dimensional and two-dimensional complexes. In the present part, we report on four one-dimensional manganese–radicals compounds $\{[Mn^{II}(NITIm)(H_2O)_2](OAc)\}_n$ (**8**), $\{[Mn^{II}(NITIm)(DMSO)_2](BPh_4)\}_n$ (**9**), $\{[Mn^{II}(NITIm)(ImH)(H_2O]NO_3\cdot H_2O\}_n$ (**10**) and $\{[Mn^{II}(NITIm)(NITImH)](ClO_4)\}_n$ (**11**).

One-dimensional compounds were obtained only with NITImH and neither with the benzimidazole substituted nitronyl nitroxide radical (Scheme 1).

In all compounds **8**–**11**, the manganese(II) ions are coordinated at least by two deprotonated nitronyl nitroxide ($NITIm^-$) acting as bis-chelating bridging ligands thus forming infinite zigzag chains. The nature of the ligands (L1 and L2) completing the coordination sphere at 6 depends on the synthetic process. In compounds **8**–**10**, the coordination sphere is completed by two water molecules (**8**) or two DMSO (**9**) or by one water molecule and one imidazole molecule (**10**) as shown on Fig. 7. Compound **11** is interesting because the coordination sphere is completed by one non-deprotonated radical (NITImH) in a mono-chelating mode so that each manganese(II) ion is surrounded by three radicals as found for the mononuclear complexes (**2**–**4**) (Fig. 8).

Within the distorted octahedral coordination sphere of the metal ion, the Mn–O and Mn–N bond distances are comparable to those found in the manganese(II) mononuclear compounds **3** and **4** (Table 4). In compound **11**, only the *mer* isomer is present (Fig. 8). As mentioned above the *mer* form is favoured here because it reduces steric crowding.

The structural features within the zigzag chain (Figs. 7 and 8) are very similar in all compounds (**8**–**11**) as illustrated by the distances between the metal ions (Mn–MnA) which vary in the range 6.335(2)–6.396(2) Å (Table 4). In compound **11**, the Δ and Λ chiral forms alternate along the chain and the non-bridging ligand (NITImH) in trans position relative to the chain direction. The counter anions OAc^- (**8**), BPh_4^- (**9**), NO_3^- (**10**) and ClO_4^- (**11**) and the crystallization water molecules (**10**) are located between the chains which are well isolated from each other.

Overall the one-dimensional compounds **8**–**11** show similar magnetic behaviour as exemplified for compound **11** in Fig. 9. On cooling, the product of the magnetic susceptibility with the temperature (χT) decreases down to a minimum (T_{min}, χT_{min}) then increases, reaching a maximum in the range 10–15 K to finally decrease at very low temperatures. This overall behaviour is similar to those observed in manganese(II)–copper(II) or manganese(II)-nitroxide chain compounds [2,3,69]. Qualitatively, the pres-

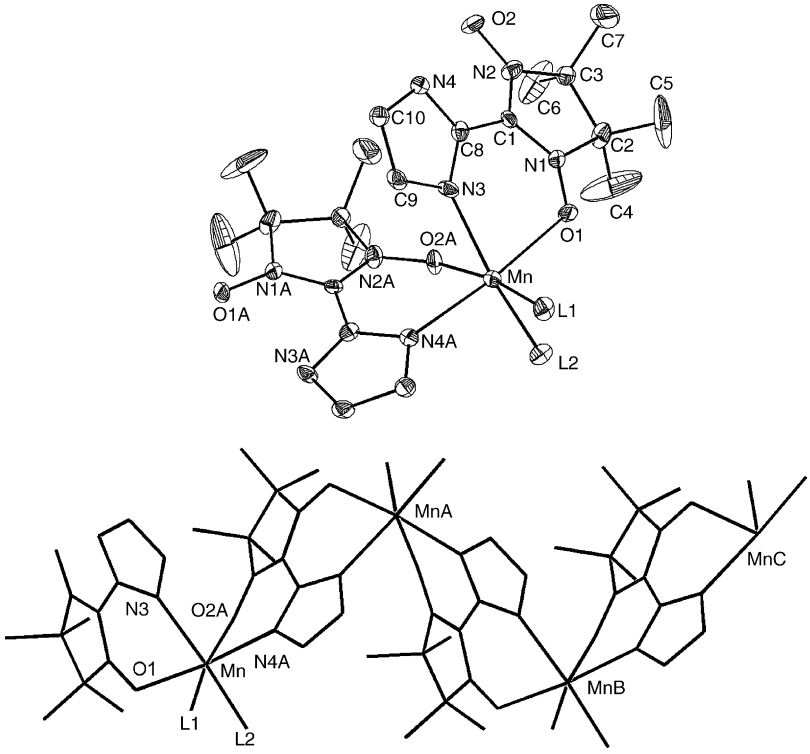

Fig. 7. View of the asymmetric unit of $\{[Mn^{II}(NITIm)(L1)(L2)]^{+}\}_n$ and fragment of the chain in compounds **8** (L1 = L2 = H_2O), **9** (L1 = L2 = DMSO) and **10** (L1 = H_2O and L2 = ImH). Reproduced with permission from Ref. [48].

ence of the minimum (T_{min}, χT_{min}) is the signature of antiferromagnetic interactions between the radical and the manganese(II) ion along the chains leading to a ferrimagnetic behaviour. The manganese-nitroxide antiferromagnetic interaction is confirmed by the χT value at 400 K lower than that of the non-coupled spin but moreover it is in agreement with the result obtained in the case of the manganese(II) mononuclear complexes $[Mn^{II}(NITBzImH)_3](ClO_4)_2$ (**2**) and $[Mn^{II}(NITImH)_3](ClO_4)_2$ (**3**). This is also confirmed by the field dependence of the magnetization at 10 K which reaches saturation to $S = 2$ (**8**–**10**) and $S = 3/2$ (**11**) ground spin state. For all compounds the magnetic susceptibility χ does not exhibit any maximum and is field dependent at low temperature. Therefore, the decrease observed in χT is probably due to saturation effects.

For all compounds **8**–**11**, we should expect two linear regimes of the temperature dependence of the inverse of the magnetic susceptibility ($1/\chi$). One high temperature regime at temperatures above T_{min} leading to negative θ and indicative of the Mn(II)–radical antiferromagnetic coupling and a second linear regime below T_{min}. Only compound **11** shows clearly both regimes (Fig. 9). Indeed, for compounds **8**–**10** the minimum (T_{min}, χ_{min}) is too high in temperature (Table 5) to allow observation of their high temperature regime in the temperature range of the study (<400 K). For all compounds **8**–**11** the low temperature regime intercepts the temperature axis at large and positive θ values within the 40–50 K range as the consequence of the ferrimagnetic behaviour.

Simulation of the magnetic properties of the chains including alternating $S = 5/2$ and 1/2 spins has been done only in the temperature range 300–100 K assuming that only the high temperature magnetic behaviour could be described by considering only the manganese–radical interactions. The interactions between the manganese(II) ions through the bridging imidazol were not considered. As well, the radical–radical interactions within the coordination sphere were neglected since the study of the mononuclear complexes have shown these to be non-relevant. For compounds **8**–**10**, the simulation of the magnetic data were achieved with a reported model [76]. A similar model including additional pendant nitroxides

Table 4
Selected bond length (Å) in compounds **8**–**11**

	Mn—O1	Mn—O2A	Mn—O3	Mn—N3	Mn—N4A	Mn—O7	Mn–MnA
8	2.181(5)	2.254(6)		2.209(7)	2.197(6)		6.396(2)
9	2.19(1)	2.25(1)		2.20(1)	2.23(1)		6.351(3)
10	2.244(8)	2.277(8)		2.201(9)	2.174(9)		6.392(2)
11	2.221(4)	2.213(3)	2.126(4)	2.182(4)	2.160(4)	2.208(4)	6.335(1)

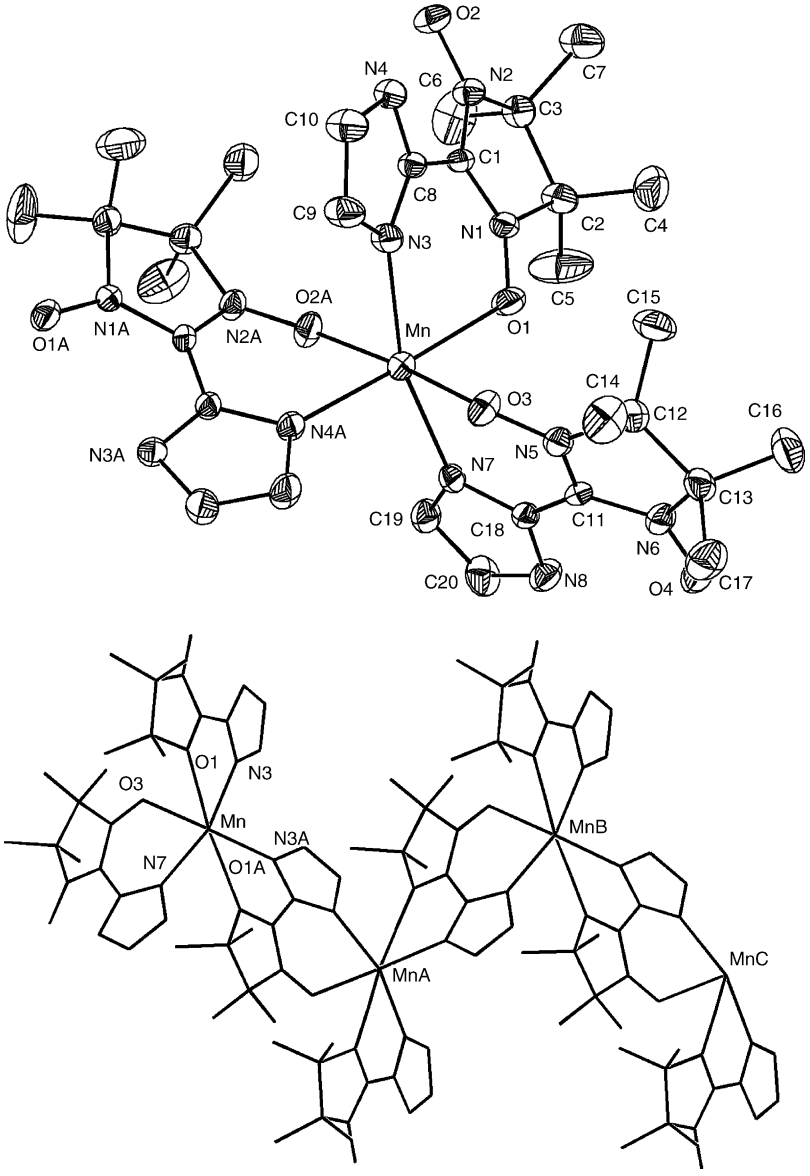

Fig. 8. View of the asymmetric unit $[Mn^{II}(NITIm)(NITImH)]^+$ and of the chain $\{[Mn^{II}(NITIm)(NITImH)]^+\}_n$ in **11**. Reproduced with permission from Ref. [48].

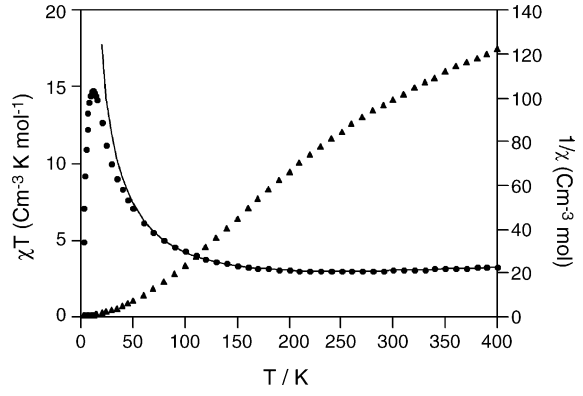

Fig. 9. Temperature dependence of χT (●) and $1/\chi$ (▲) for compound $\{[Mn^{II}(NITIm)(NITImH)](ClO_4)\}_n$ (**11**). The solid lines represent the best fit of the data with values reported in the text. Reproduced with permission from Ref. [48].

was developed in the case of compound **11**. The coupling constant (50–80 K) found for compounds **8**–**9** compares well with those observed in the mononuclear complexes (Table 5).

The temperature dependence of the ac magnetic susceptibility recorded at 116 Hz in 0.1 G field and at low temperatures shows deviation from the Curie law below 10 K. These effects are well understood as being the consequence of antiferromagnetic interactions. However, on cooling, χ' increases sharply in the range 4.5 K (Fig. 10) which is the signature of ferromagnetic interactions. At lower temperatures (<2.4 K) the ac susceptibility decreases and tends to an extrapolation of the curve observed above 5 K.

The low field (0–3 G) magnetization $M(H)$ shows a strong initial variation which is consistent with the high value of χ'. On increasing the field strength, one observes a saturation behaviour corresponding only to a small fraction of the total

Table 5
Parameters relative to magnetism in compounds **8**–**11**

	8	**9**	**10**	**11**
χT at 400 K ($cm^3\ mol^{-1}\ K$)	4.26	4.00	4.75	3.3
T_{min} (K)	380(5)	378(5)	380(5)	252(5)
χT_{min} ($cm^3\ mol^{-1}\ K$)	4.22	3.83	3.75	2.96
T_{max} (K)	10(2)	12(2)	14(2)	11(2)
J_1[a] (cm^{-1})	−45(4)	−43(3)	−46(4)	−49(4)
J_2[a] (cm^{-1})				−86(5)
T_c (K)	4.8	1.9	4.3	4.5

[a] $H = -2JS_iS_j$.

expected magnetization. These two features are also characteristic of the onset below 4.5 K of a weak ferromagnetic component. Below 4.2 K, a hysteresis loop appears whose coercive field increases rapidly to reach 300 G at 0.08 K. The initial value of the magnetic susceptibility at 0.8 K is much weaker than at 4.2 K. On increasing the magnetic field one sees an upward curvature of the magnetization which indicates that the antiferromagnetic interaction is progressively overcome by the magnetic field. The magnetization at saturation (hysteresis loop) indicates that the ferromagnetic component is very weak since it corresponds to only 1.5% of the expected saturation magnetization.

The onset of a remnant magnetization loop is confirmed by the difference between the "zero-field-cooled" (ZFC) and the "field-cooled" magnetization curves (Fig. 11). On examining the data displayed on this figure, the ordering temperature can be determined to be in the range (1.9–4.5 K) for compounds **8**–**11** (Table 5) consistent with the ac measurements.

Canting is obviously at the origin of the low temperature ordering in these compounds **8**–**11**. Such weak ferromagnetism behaviour is also observed in structurally related 1D materials [77,78] as the results of in-chain and inter-chain interaction. Although manganese(II) is usually highly isotropic, the coordination spheres within the chains (**8**–**11**) are distorted in different ways leading to magnetically inequivalent adjacent metal ions [78]. These ferrimagnetic chains involving non-equivalent metal ions are weakly antiferromagnetically coupled. Therefore, at low temperature where these interactions are operative, the compounds exhibit a non-vanishing weak magnetic moment [77,78]. It is interesting to note that compounds **8**–**11** exhibit the same behaviour but with small differences in ordering temperatures. This reflects the differences in inter-chain spacing due to the presence of counter anions with different size, due to different ancillary ligands (L1, L2) and due to solvent. This is particularly obvious for $\{[Mn^{II}(NITIm)(DMSO)_2](BPh_4)\}_n$ (**9**) which has the lower T_c (1.9 K) (Table 5).

Compounds **8**–**12** are the only examples of 1D molecular magnetic materials involving nitroxide free radicals and transition metal ions in which the coordination sphere is free of ancillary electron-withdrawing groups. These compounds are magnets exhibiting ordering temperatures below 5 K. Although difficult to control, the coordination chemistry of these ligands is rich. Of particular interest is compound **11** where only radicals are present in the coordination sphere and which may be viewed as the precursor of 2D or 3D metal-nitroxide compounds.

3.2.5. *Two-dimensional complexes [47,49,52]*

Reaction of any of the ligands described in Scheme 1 with manganese(II) acetate gave upon addition of most

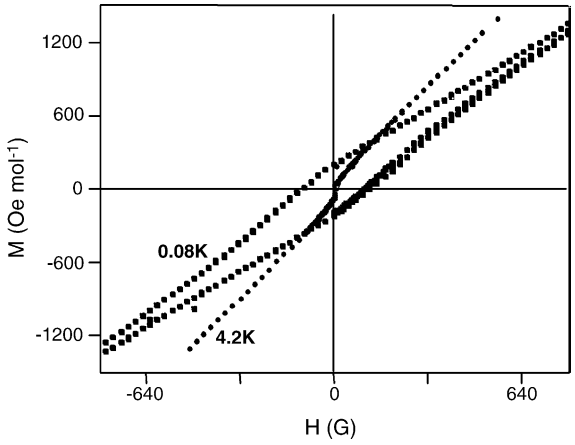

Fig. 10. Cycled field dependence of the magnetization at 4.2 K and 0.08 K for compound **11**. Reproduced with permission from Ref. [48].

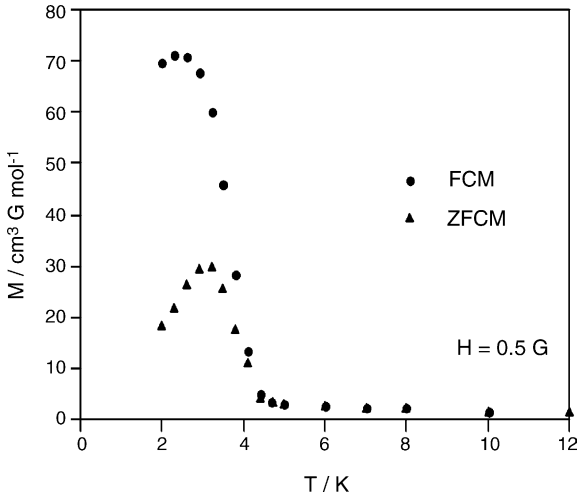

Fig. 11. Zero-field cool (▲) and field cool (●) magnetization for compound **11**. Reproduced with permission from Ref. [48].

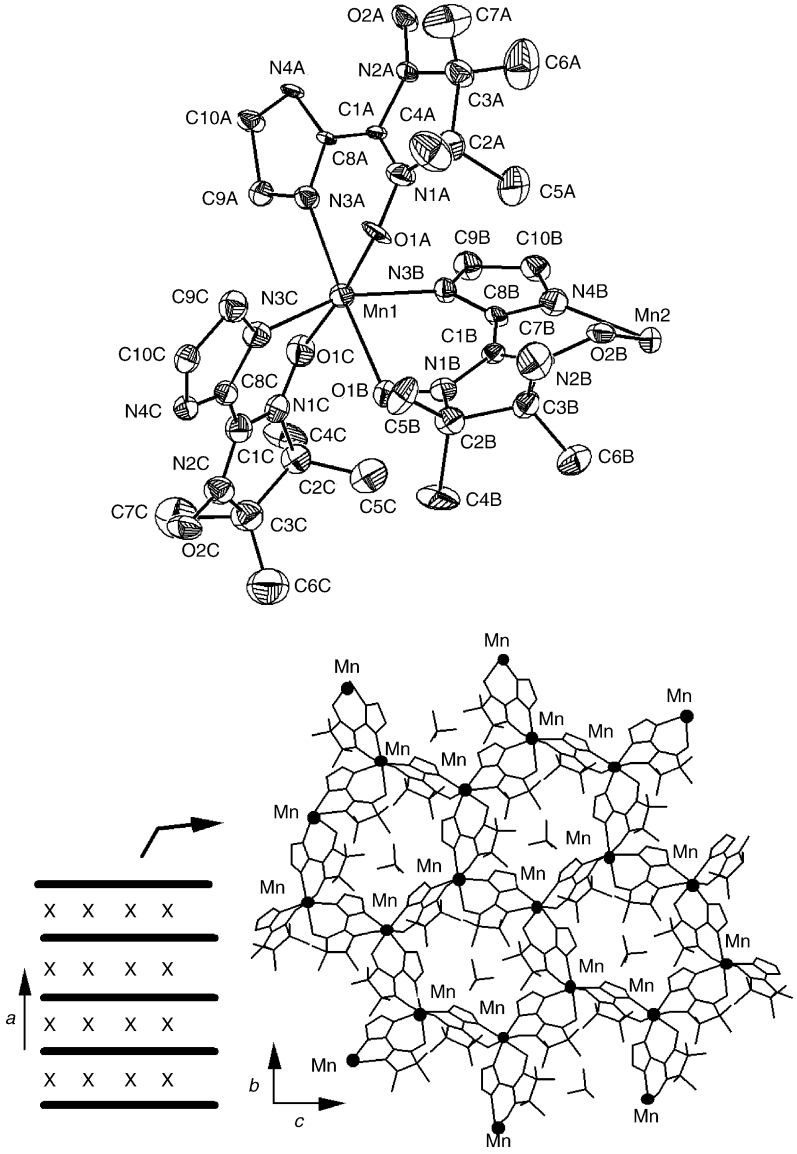

Fig. 12. View of the asymmetric unit and of the honeycomb like structure of compound $\{[Mn^{II}_2(NITIm)_3](ClO_4)\}_n$ (**12**). Reproduced with permission from Ref. [47].

counteranions (X^-), compounds which analysed satisfactory as $\{[Mn^{II}_2(radical)_3]X\}_n$ (radical = $NITIm^-$, $NITBzIm^-$, $NITMeBzIm^-$, $NIT(NO_2)BzIm^-$). Different counter ions (X = ClO_4, BF_4, PF_6, BPh_4, alkylsulfate) were used successfully. It did not work only in the case of the NO_3^- and Cl^- counter anions for which one-dimensional compounds (**8** and **10**) were characterized with NITImH. The crystal structure was solved from single crystal X-ray diffraction in the case of the derivative of NITImH radical with perchlorate anions. Compound $\{[Mn^{II}_2(NITIm)_3](ClO_4)\}_n$ (**12**) consists of 2D Mn–radical networks with a honeycomb like structure in which each manganese is coordinated to three radicals (Fig. 12). The perchlorate anions are located between the 2D layers $[Mn^{II}_2(NITIm)_3]_n^-$. The compound is best viewed as a lamellar compound with layers separated by 10.32(1) Å (Fig. 12).

Within the 2D layers the Mn(II) environment with three coordinated radicals is reminiscent of those found in mononuclear compounds **3**–**4** and in the one-dimensional compound **11** except that here the three radicals are deprotonated ($NITIm^-$) and bridging as well. The Mn–O and Mn–N (Table 6) compare well with those found for the mononuclear **2**–**4** (Table 1) and the one-dimensional compounds **8**–**11** (Table 4). The distances between the two nearest manganese(II) atoms is 6.3(2) Å which compares well with those found in the one-dimensional compounds (**8**–**11**). As observed in compound **11** only the *mer* isomer is present in compounds **12** (Fig. 7) probably again due to the steric crowding. Within a 2D layer the alternating Δ and Λ chiral forms are found as expected for such a 2D network built from bis-chelating ligands as previously observed in oxalato compounds [79].

Table 6
Selected Bond Lengths (Å) in compound $\{[Mn^{II}_2(NITIm)_3](ClO_4)\}_n$·(**12**)

Mn1		Mn2	
Mn1–O1A	2.18(2)	Mn2–O2A	2.19(2)
Mn1–O1B	2.29(2)	Mn2–O2B	2.20(2)
Mn1–O1C	2.16(2)	Mn2–O2C	2.23(2)
Mn1–N3A	2.22(2)	Mn2–N4A	2.17(2)
Mn1–N3B	2.26(2)	Mn2–N4B	2.17(3)
Mn1–N3C	2.11(3)	Mn2–N4C	2.20(2)
Mn1–Mn2	6.3(2)		

XRD powder patterns carried on all compounds of the series $\{[Mn^{II}_2(radical)_3]X\}_n$ (radical = $NITIm^-$, $NITBzIm^-$, $NITMeBzIm^-$, $NIT(NO_2)BzIm^-$ and X = ClO_4, BF_4, PF_6, alkylsulfate) are consistent with the same lamellar structure but with different spacing between the layers.

The temperature dependence of the magnetic behaviour for these layered compounds is exemplified in the form of the temperature dependence of the χT product in Fig. 13. For each compound, on cooling, the χT product increases continuously and reaches a maximum at a temperature depending on the counter anions and on the chemical substituents on the imidazole or benzimidazole rings (Fig. 13). This temperature dependence is characteristic of the ferrimagnetic behaviour due to the antiferromagnetic interactions between the Mn(II) ions and the nitroxide radicals within the $\{[Mn^{II}_2(NIT\text{-}Im)_3]\}_n$ sheets in agreement with the results shown above for the mononuclear compounds (**2**–**3**) and the one-dimensional compounds (**8**–**11**).

Examination of the ZFCM and FCM curves shows the onset of long-range magnetic ordering below 1.4 K for the imidazole derivatives $\{[Mn^{II}_2(NITIm)_3]\ X\}_n$ while the benzimidazole derivatives $\{[Mn^{II}_2(NIT\text{-}Bz(R,R')Im)_3]\ X\}_n$ display higher ordering temperatures up to 60 K in some cases (Fig. 14). As expected, the highest Curie temperatures are obtained when small counter ions are used that is ClO_4, PF_6, BF_4.

For most compounds, cyclic magnetization measurements show an hysteresis loop below the Curie temperature. In the case of the compounds obtained with the benzimidazol substituted nitronyl nitroxide ($NITBzIm^-$, $NITBzMeIm^-$ and $NITBz(NO_2)Im^-$), the magnetization at saturation and the coercive field were found to be also tuned by the R substituent on the benzimidazol ring (Scheme 1) as shown for compounds $\{[Mn^{II}_2(NITBzIm)_3](ClO_4)\}_n$ (**13**) $\{[Mn^{II}_2(NITMeBzIm)_3](ClO_4)\}_n$ (**16**) $\{[Mn^{II}_2(NIT(NO_2)BzIm)_3](ClO_4)\}_n$ (**17**) in (Fig. 15). However, all compounds have magnetization at saturation below the value of 7 μB expected for two manganese(II) ions ($S = 5/2$) and three radicals ($S = 1/2$) antiferromagnetically coupled. The lowest value (0.22 μB at 85 mK) is observed for the NITImH derivative $\{[Mn^{II}_2(NITIm)_3](ClO_4)\}_n$ (**12**) while the highest (6 μB at 2 K) is observed for the analogue compound with NITBzImH $\{[Mn^{II}_2(NITBzIm)_3](ClO_4)\}_n$ (**13**) (Fig. 15).

As for the 1D compounds (**8**–**11**) the low value of the magnetization at saturation is indicative of weak ferromagnetism in the 2D compounds and may be ascribed to canting. Indeed, we may expect that the 2D layer interacts antiferromagnetically but, because the two manganese(II) ions of the asymmetric unit (Fig. 12) are crystallographically independent and magnetically independent, this results in a weak residual magnetic moment.

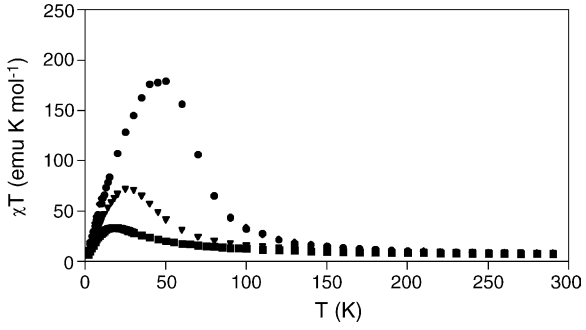

Fig. 13. Temperature dependence of χT for $\{[Mn^{II}_2(NITBzIm)_3]X\}_n$ compounds with different of anions. (●) Compound **13** (X = ClO_4^-). (▼) Compound **14** (X = BPh_4^-). (■) Compound **15** (X = dodecylsulfate).

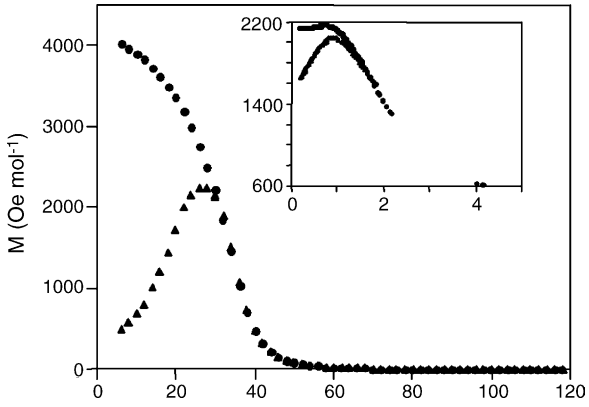

Fig. 14. Temperature dependence of the magnetization for compound $\{[Mn^{II}_2(NITIm)_3](ClO_4)\}_n$ (**12**) in insert and for compound $\{[Mn^{II}_2(NITBzIm)_3](ClO_4)\}_n$ (**13**). Reproduced with permission from Ref. [47].

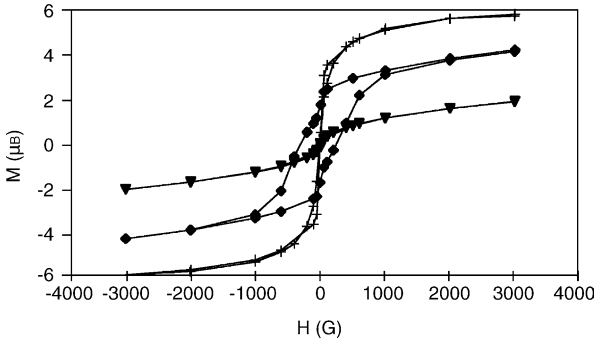

Fig. 15. Cycled field dependence of the magnetization at 2 K for compound$\{[Mn^{II}_2(radical)_3](ClO_4)\}_n$ (+) Compound **13** (radical = $NITBzIm^-$). (▼) Compound **16** (radical = $NIT(NO_2)BzIm^-$). (■) Compound **17** (radical = $NITMeBzIm^-$).

3.3. Lanthanide compounds [43,51,53,54,80]

One of our prior interests in lanthanide coordination chemistry arose from their known ability for high coordination numbers and this may be a key point for the design of tridimensional metal-nitroxide networks. Secondly, prior to this work the Gd^{III}–radical magnetic interaction was known to be ferromagnetic by nature. Therefore, after the 2D manganese(II) compounds, it was appealing to think that the lanthanides would give 3D compounds with ferromagnetic behaviour.

Our finding that the Gd^{III}–radical interactions may be antiferromagnetic greatly undetermined this confidence. Therefore, with the aim to better understand the factors which may affect the sign of the magnetic interaction, we undertook the synthesis and the magneto-structural studies of many Gd(III) complexes in which the type and the number of nitroxide radicals around the metal centre were varied. For comparison purposes, we also synthesized the analoguous complexes with La(III) and Eu(III). Spectroscopic studies have also been done first as a support to the magnetic study but also to investigate their optical properties in the frame of our interest for magneto-optical materials.

Complexes of formula $[Ln(radical)_4]^{3+}$ (**18**–**21**) were obtained with the NITMeBzImH and NITBzImH radicals and the perchlorates of lanthanide [Gd(III), La(III), Dy(III)]. The lanthanide ion [Ln = Gd(**18**, **20**) or La (**19**, **21**)] is eight-coordinated by four chelating nitronyl nitroxide radicals NIT-

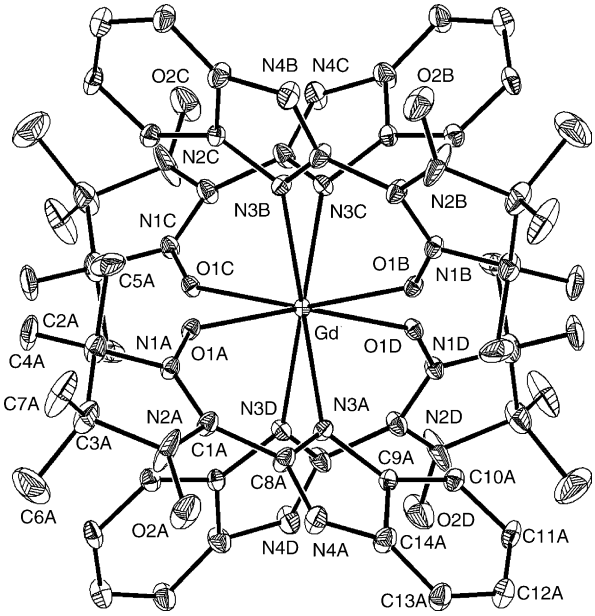

Fig. 16. Molecular structure of complex $[Gd^{III}(NITBzImH)_4]^{3+}$ (**18**). Reproduced with permission from Ref. [51].

BzImH (**18**, **19**) or NITMeBzImH (**20**, **21**) as exemplified for **18** in Fig. 16 [51,54]. The neutrality of the complexes is achieved by non-coordinated perchlorate anions and all compounds **18**–**21** contain crystallization water and THF molecules. Therefore, the cations $[Ln(radical)_4]^{3+}$ are well

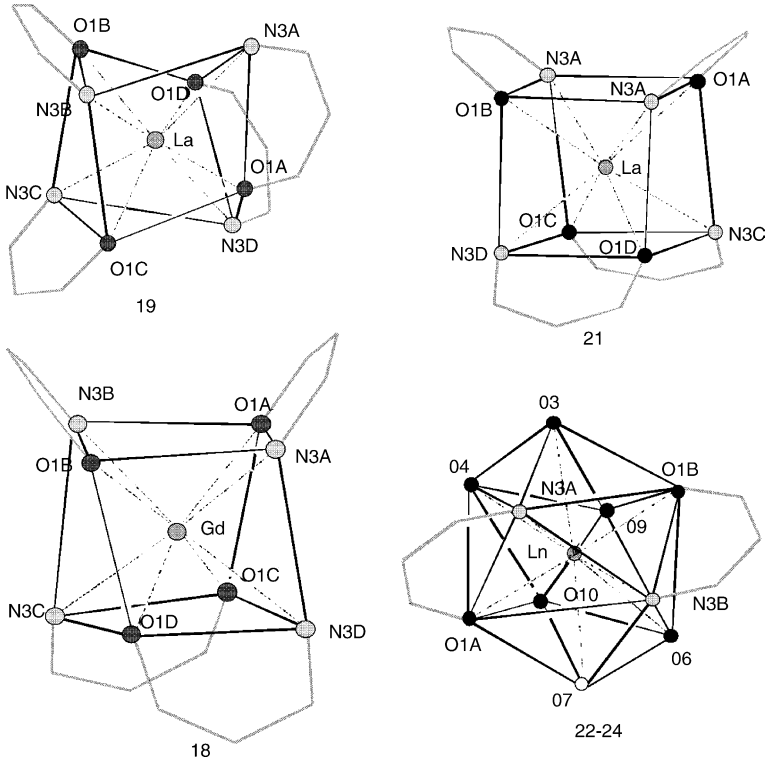

Fig. 17. Schematic representations drawn from crystal structure features showing the coordination polyhedron for **18**–**21** and **22**–**24**. For clarity, only the atoms involved in the chelate ring and in the coordination sphere are shown. Reproduced with permission from Ref. [51].

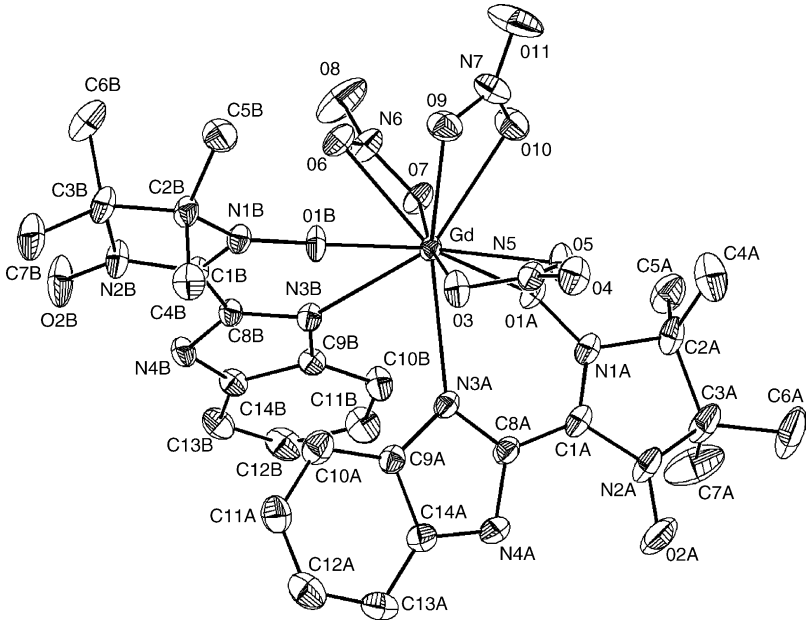

Fig. 18. Molecular structure of complex $[Gd^{III}(NITBzImH)_2(NO_3)_3]$ (**22**). Reproduced with permission from Ref. [51].

isolated from each other from the magnetic point of view. As for the transition metal compounds, the $[Ln(radical)_4]^{3+}$ fragments show different stereoisomers owing to the $M(X–Y)_4$ coordination pattern exhibiting distorted cube (**18** and **21**) or dodecahedron (**19**) coordination polyhedron (Fig. 17).

With the nitrate anions, only two nitronyl nitroxide radicals are bound to the lanthanide ion. The coordination sphere is completed up to 10 by the oxygen atoms of three coordinated nitrate ions to give compounds of formula $[Ln(radical)_2(NO_3)_3]$ [Ln = Gd(**22**), La (**23**) or Eu(**24**)] as shown for **22** in Fig. 18.

In the two previous series of complexes, the lanthanide(III) ion was coordinated to four (**18**–**21**) or two (**22**–**24**) radicals. The third series of compounds **25**–**31** consists of $[Ln(radical)(hfac)_3]$ entities in which the lanthanide ion [Ln = Gd(**25**, **27**, **29**, **31**) or Eu(**26**, **28**, **30**)] is bound to only one nitronyl nitroxide radical NITBzImH (**25**–**26**) and NITPy (**31**), or one imino nitroxide IMBzImH (**27**, **28**) or IMPy (**29**, **30**) as shown in Fig. 19. The coordination sphere is completed up to eight by the oxygen atoms of three hexafluoroacethylacetonato (hfac) ligands. Compounds $[Gd(NITPy)(hfac)_3]$ (**29**) [37] and $[Gd(IMPy)(hfac)_3]$ (**31**) [81] were also reported elsewhere.

All complexes **18**–**31** exhibit bond distances and angles within the range generally observed in related complexes [37,61] (Table 7).

The temperature dependence of the magnetic susceptibilities of the europium(III) compounds were not quantified but they all evidenced the thermal depopulation of the magnetic excited states to the diamagnetic ground state $^7F_0$ when lowering the temperature.

The study of the temperature dependence of the magnetic susceptibility of the lanthanum(III) compounds (**19**, **21**, **23**) allowed the quantification of intra and intermolecular radical–radical magnetic interactions which were found to be negligible in **19** and **21**; and assumed to be so in all perchlorate derivatives and particularly in the related gadolinium(III) complexes **18** and **20** (Table 7) [51,54]. In contrast, for the nitrate compounds (**23**), sizeable antiferromagnetic radical–radical interactions (Fig. 20) could be quantified using a dimer model with $J_{rad1–rad2} = -1.1\ cm^{-1}$ $[H = -2J_{rad1–rad2}(S_{rad1}S_{rad2})]$ [43,54]. Since the intermolecular contacts are greater than 3.4 Å, these radical–radical interactions are intramolecular either within the coordina-

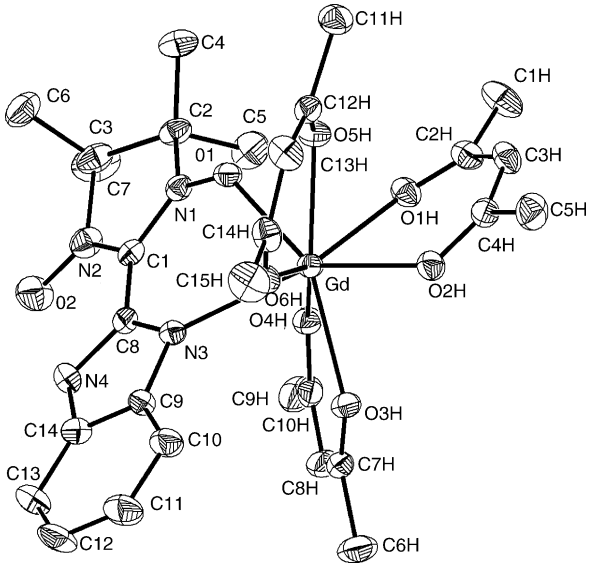

Fig. 19. View of complex $[Gd^{III}(hfac)_3$ NITBzImH] (**25**). Reproduced with permission from Ref. [51].

Table 7
Selected bond lengths (Å) in compounds (**18**–**31**)

		Ln–N1	Ln–O1	Ln–N3	O1–N1	O2–N2
18	$[Gd^{III}(NITBzImH)_4]^{3+}$		2.352(6)	2.582(9)	1.27(1)	1.27(1)
19	$[La^{III}(NITBzImH)_4]^{3+}$		2.446(7)	2.722(7)	1.29(1)	1.26(1)
21	$[La^{III}(NITMeBzImH)_4]^{3+}$		2.48(2)	2.68(3)	1.28(3)	1.29(3)
22	$[Gd^{III}(NITBzImH)_2(NO_3)_3]$	Radical A	2.405(3)	2.577(3)	1.291(4)	1.274(5)
		Radical B	2.365(3)	2.585(3)	1.282(4)	1.274(5)
23	$[La^{III}(NITBzImH)_2(NO_3)_3]$	Radical A	2.502(4)	2.731(5)	1.302(6)	1.273(7)
		Radical B	2.462(4)	2.697(5)	1.282(6)	1.283(7)
24	$[Eu^{III}(NITBzImH)_2(NO_3)_3]$	Radical A	2.369(3)	2.590(7)	1.294(8)	1.25(1)
		Radical B	2.413(3)	2.598(6)	1.280(8)	1.263(9)
25	$[Gd^{III}$ NITBzImH$(hfac)_3]$		2.342(3)	2.570(3)	1.286(4)	1.273(4)
26	$[Eu^{III}$ NITBzImH$(hfac)_3]$		2.359(3)	2.593(3)	1.287(4)	1.272(5)
27	$[Gd^{III}$ IMBzImH$(hfac)_3]$	2.599(5)		2.519(5)		1.261(7)
28	$[Eu^{III}$ IMBzImH$(hfac)_3]$	2.621(2)		2.533(2)		1.255(3)
29	$[Gd^{III}$ IMPy$(hfac)_3]$	2.555(4)		2.557(4)		1.269(6)
30	$[Eu^{III}$ IMPy$(hfac)_3]$	2.557(2)		2.568(2)		1.273(4)
31	$[Gd^{III}$ NITPy$(hfac)_3]$ [37]		2.322(7)	2.614(9)	1.319(8)	1.266(9)

tion sphere or through the lanthanum as proposed elswere [63].

The gadolinium(III) compounds of the first two series (**18**, **20**, **22**) show an overall antiferromagnetic behaviour (Figs. 20 and 21). At 300 K, χT has values close to those expected for the independent spins [9.45 (**9**), 9.40 (**11**) and 8.58 (**13**)] and decreases continuously on cooling for the three compounds (Figs. 21 and 22). This antiferromagnetic behaviour is not due to dominant radical–radical interactions as the lanthanum(III) compounds clearly showed that they are weak (**23**) or even negligible (**19**, **21**). Moreover, high magnetic field measurements of their magnetization (0–5.5 T) have shown that the magnetic behaviour of these gadolinium(III) compounds (**18**, **20** and **22**) is unambiguously due to antiferromagnetic Gd^{III}–radical interactions. This was confirmed by simulation of the temperature dependence of the magnetic susceptibility ($g = 2$, $H = -JS_iS_j$). The best fit parameters are as follows: $J_{Gd–rad} = -1.8\,cm^{-1}$ (**18**); $J_{Gd–rad} = -3.8\,cm^{-1}$ (**20**) and $J_{Gd–rad1} = -4.05\,cm^{-1}$ and $J_{Gd–rad2} = -0.80\,cm^{-1}$(**22**) (Table 8).

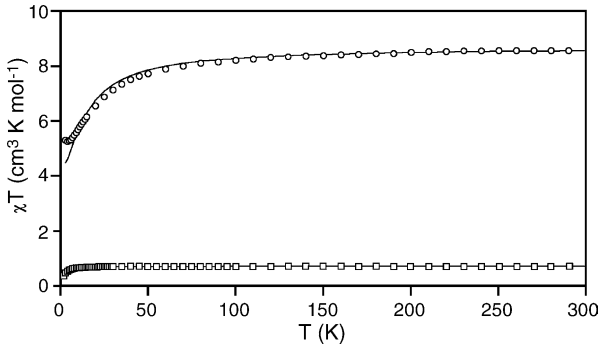

Fig. 20. Temperature dependence of χT for $[La^{III}(NITBzImH)_2(NO_3)_3]$ (**23**) (□) and compound $[Gd^{III}(NITBzImH)_2(NO_3)_3]$ (**22**) (◯). The solid lines represent the best fit of the data with values in the text. Reproduced with permission from Ref. [51].

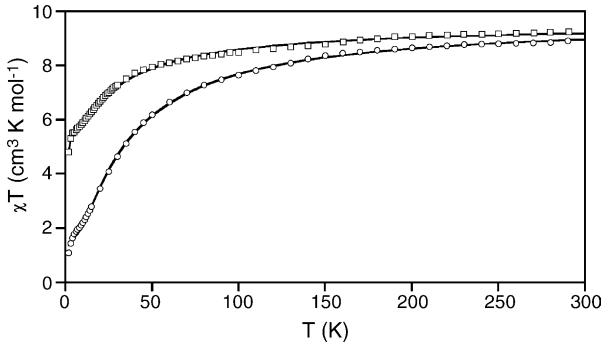

Fig. 21. Temperature dependence of χT for compounds $[Gd^{III}(NITBzimH)_4]\cdot(ClO_4)_3\cdot 2THF\cdot 1H_2O$ (**18**) (□) and $[Gd^{III}(NITMeBzimH)_4]\cdot(ClO_4)_3\cdot 2THF\cdot 1H_2O$ (**20**) (◯). The solid lines represent the best fit of the data with values reported in the text. Reproduced with permission from Ref. [51].

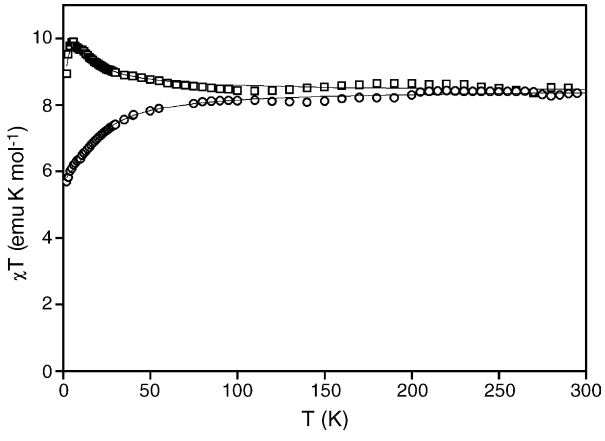

Fig. 22. Temperature dependence of $\chi_m T$ for $[Gd^{III}(hfac)_3NITBzimH]$ (**25**) (□) and for $[Gd^{III}(hfac)_3$ IMBzImH] (**27**) (◯). Solid lines are calculated with the parameters reported in the text. Reproduced with permission from Ref. [51].

Table 8
Value of the Gd^{III}–radical magnetic interactions for this work and related compounds reported in the literature

	Compounds	J_{Gd-rad} (cm^{-1})
18	$[Gd(NITBzImH)_4]\cdot(ClO_4)_3\cdot 2THF\cdot 2H_2O$	−1.8
20	$[Gd(NITMeBzImH)_4]\cdot(ClO_4)_3\cdot 2THF\cdot 1H_2O$	−3.8
22	$[Gd(NITBzImH)_2(NO_3)_3]$	−4.05 and −0.80
25	$[Gd(NITBzImH)(hfac)_3]$	+1.7
27	$[Gd(IMBzImH)(hfac)_3]$	−2.6
29	$[Gd(IMPy)(hfac)_3]$	−1.9
31	$[Gd(NITPy)(hfac)_3]$	+1.51[a]
	$[Gd(NITtrz)_2(NO_3)_3]$	+6.1[b]
	$[Gd(NITPh)_2(hfac)_3]$	+1.0[c]
	$[Gd(NITPr)(hfac)_3]$	+0.25[d]

[a] Ref. [37].
[b] Ref. [61,63].
[c] Ref. [82].
[d] Ref. [83].

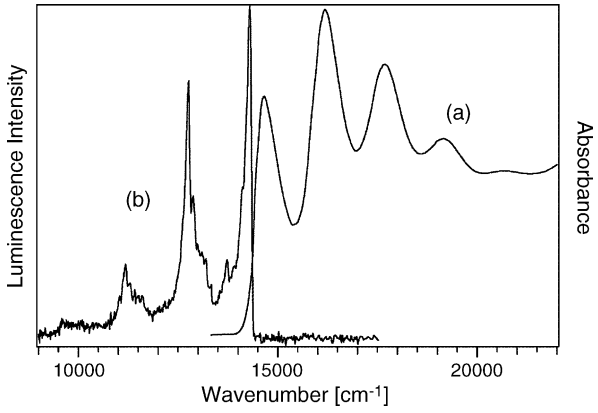

Fig. 23. Single-crystal absorption (a) and luminescence (b) spectra of $[Gd^{III}(hfac)_3NITBzimH]$ (**25**) at 5 K. Reproduced with permission from Ref. [43].

Antiferromagnetic Gd^{III}–radical interactions were also found in the case of the gadolinium compounds [Gd(radical)(hfac)$_3$] with the imino nitroxide radicals IMBzImH and IMPy [(**27**) $J_{Gd-rad} = -2.6\,cm^{-1}$ and (**29**) ($J_{Gd-rad} = -1.9\,cm^{-1}$) [43]. In contrast, ferromagnetic interactions are found for the nitronyl nitroxide complexes **25** and **31** (Fig. 22); $J_{Gd-rad} = +1.7\,cm^{-1}$ for **25** [43] is a value comparable to that reported previously for compound **31** ($J_{Gd-rad} = +1.5\,cm^{-1}$) [37].

Among the gadolinium(III) complexes presented here only [Gd(NITBzImH)(hfac)$_3$] (**25**) and [Gd(NITPy)(hfac)$_3$] (**31**) exhibit a ferromagnetic Gd^{III}–radical interaction. This is evidence that magnetic coupling between gadolinium(III) and free radical ligands [37,61,82,83] is not intrinsically ferromagnetic as was assumed previously and this has been confirmed by other results [84,85]. Therefore, the previous model based on electron transfer between the magnetic orbital of the free radical and the empty orbitals of the gadolinium(III) ion (5d or 6s) resulting in stabilization of the higher multiplicity ground spin state according to Hund's rule [83,86] is no longer universally applicable.

However, no clear trend is observed which may relate the Gd^{III}–radical magnetic interaction to the molecular structure. When looking at the [Gd(radical)(hfac)$_3$] series (**25**, **27**, **29**) the apparent trend is that the Gd^{III}–radical coupling becomes more antiferromagnetic as the Gd^{III}–radical distance increases [**25**: $J_{Gd-rad} = +1.7\,cm^{-1}$, Gd–O1(NO) = 2.342(3) Å; **27**: $J_{Gd-rad} = -2.6\,cm^{-1}$, Gd–N1(imino) = 2.599 Å; **29**: $J_{Gd-rad} = -1.9\,cm^{-1}$, Gd–N1(imino) = 2.555(4) Å]. This is not strictly the case when comparing them to the nitrato complex [Gd(NITBzImH)$_2$(NO$_3$)$_3$] (**22**: $J_{Gd-rad1} = -4.05\,cm^{-1}$ and $J_{Gd-rad2} = -0.80\,cm^{-1}$, Gd–O1A(NO) = 2.405 cm^{-1} and Gd–O1B(NO) = 2.365(3) Å). Moreover, it does not work at all when comparing the nitrato complex **22** to a structurally similar compounds obtained with a triazole substituted nitronyl nitroxide radicals (Scheme 2) and exhibiting a ferromagnetic Gd^{III}–radical coupling [61,63]. In these latter case, the trend would be that the Gd^{III}–radical coupling becomes ferromagnetic when the Gd^{III}–radical bond lengths increases [Gd–O1 = 2.460(15) Å and Gd–O4 = 2.430(15) Å, $J_{Gd-rad} = +6.1\,cm^{-1}$] [61,63]. These observations strongly indicate that the sign and magnitude of the Gd^{III}–radical interactions depend on the detailed electronic structure and on bonding characteristics involving the lanthanide ions, the radical ligands and the ancillary ligands.

To have a deeper insight on these electronic features and their relationship with the magnetic properties, the spectroscopic properties of the lanthanide compounds were also investigated. As these properties have been recently fully reviewed [87] only the main results are reported hereafter.

The excited states of the coordinated radicals are only weakly affected by the metal centre. Therefore, all gadolinium(III) and europium(III) complexes (**18**–**31**) show emission and absorption spectra very similar to those of their uncoordinated radicals as shown for compound **25** in Fig. 23, and as observed for most lanthanides complexes and d-block metals complexes with nitroxide radicals [88–90]. Fine analysis of the spectra of the gadolinium(III) and europium(III) complexes (**18**–**31**) shows subtle differences which depend on the type and number of coordinated radical and also on the ancillary ligands.

In the case of the europium(III) complexes, the luminescence was found to be tuned by the coordinated radical (Fig. 24). For example, for the nitrato compound [Eu(NITBzImH)$_2$(NO$_3$)$_3$] (**24**) the radical-centred luminescence dominates and the f–f luminescence of the europium(III) ion is almost completely switched-off while the opposite effect is observed for the hexafluoroacetylacetonato compound [Eu(IMBzImH)(hfac)$_3$] (**30**) (Fig. 24). The balance of the phenomena depends on the energy difference between the radical centred band and the f–f transition of europium(III) and this explains qualitatively the intensity differences observed in Fig. 24.

The signatures of magnetic effects in the optical spectra of the lanthanide complexes are generally not obvious

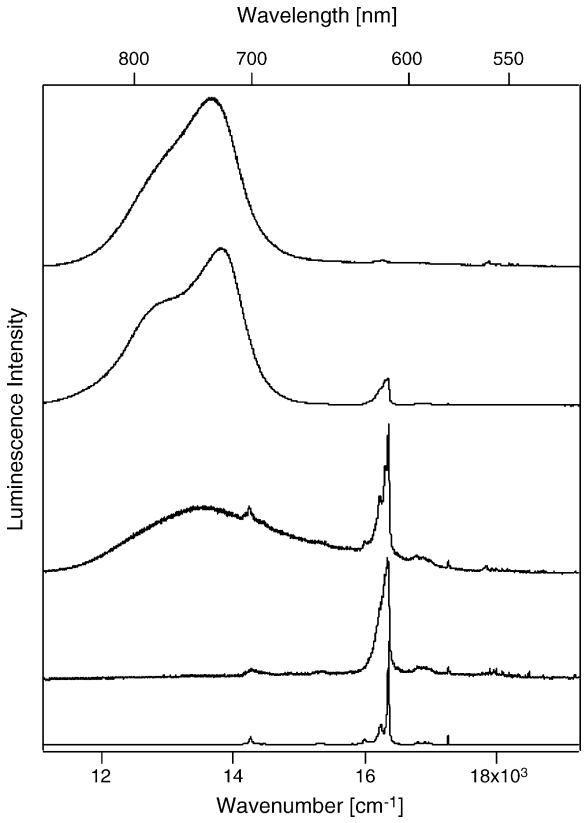

Fig. 24. Comparison of luminescence spectra of Eu(III) complexes with radical ligands. Top to bottom: $[Eu^{III}(NitBzimH)_2(NO_3)_3]$ (1b) (290 K), $[Eu^{III}(hfac)_3NitBzimH]$ (2b) (290 K), $[Eu^{III}(hfac)_3ImBzimH]$ (3b) (5 K) and $[Eu^{III}(hfac)_3IMPy]$ (4b)(5 K). The lowest trace is $Eu(hfac)_3{\cdot}2H_2O$ (5 K) given as a reference compound. Reproduced with permission from Ref. [43].

in contrast to the d-block complexes where the ground-state exchange splittings can be determined from luminescence spectra [91]. However, the analysis of the optical spectra in the light of the magnetic behaviour allowed us to conclude that both the energy difference between the ground and emitting states and the detailed band shape of the luminescence spectra can be qualitatively correlated with the sign of the lanthanide–radical exchange interaction. An appealing suggestion is that in some cases the energy difference between the singly-occupied orbital of the radical (SOMO) and the empty 5d orbital on the lanthanide centre leads to an increase of the SOMO to 5d electron transfer energy, which was previously postulated to be a determining factor for the ferromagnetic Gd^{III}–radical [or Cu^{II}–Gd^{III}] interaction [37,61,82,83,92]. If this energy increases sufficiently, the magnetic interaction becomes antiferromagnetic.

4. Conclusions and perspectives

This review illustrates the versatility of bis-chelating nitroxide free radicals in magnetic engineering. They are particularly promising spin carriers for designing extended exchange-coupled networks as illustrated with the one-dimensional and two-dimensional manganese(II) compounds exhibiting magnet like behaviour with relatively high Curie temperature in the case of the 2D systems. Moreover, these 2D-complexes are appealing for the development of intercalation compounds. Work is also in progress with other transition metal ions. For example, compounds of cobalt(II) were recently found to give higher Curie temperatures. Special attention has been placed on the design of three-dimensional structures. As demonstrated by previous work on oxalate [68,70] this involves the control over the chirality of the metal centre which may be achieved using recently designed chiral nitroxides.

The lanthanide compounds reported in this review have proved to be important to give new insight in the sign of the Gd(III)–radical magnetic interaction. All lanthanide complexes described in this paper are isolated species but the future challenge is the design of extended 2D or 3D structures. The study of their optical properties provided some information on the relationship between electronic structure and magnetism. Moreover, the discovery that they exhibit luminescence is promising for the development of novel multifunctional materials with magneto-optical properties.

Acknowledgements

We would thank all our co-workers on synthesis, magnetic theory, low temperature magnetic measurements and optical studies: Christophe Lescop, Karine Fegy, Elie Belorizky, Carley Paulsen, Christian Reber, Guillaume Bussière, Rémi Beaulac. This work was supported by the Commissariat à l'Energie Atomique (CEA), the Centre de la Recherche Scientifique (CNRS), the European Community through TMR programmes, the Centre Jacques Cartier and the Commission Permanente de Coopération Franco-Québécoise.

References

[1] A. Caneschi, D. Gatteschi, R. Sessoli, P. Rey, Acc. Chem. Res. 22 (1989) 392.
[2] A. Caneschi, D. Gatteschi, P. Rey, Prog. Inorg. Chem. 39 (1991) 331.
[3] H. Iwamura, K. Inoue, in: J.S. Miller, M. Drillon (Eds.), Magnetism: Molecules to Materials II. Molecule-Based Materials, Wiley–VCH, Weinheim, Germany, 2001, p. 61.
[4] H. Oshio, T. Ito, Coord. Chem. Rev. 198 (2000) 329.
[5] R. Ziessel, G. Ulrich, R.C. Lawson, L. Echegoyen, J. Mater. Chem. 9 (1999) 1435.
[6] S.S. Eaton, G.R. Eaton, Coord. Chem. Rev. 26 (1978) 207.
[7] M. Kinoshita, P. Turek, M. Tamura, K. Nozawa, D. Shiomi, Y. Nakazawa, M. Ishikawa, M. Takahashi, K. Awaga, T. Inabe, Y. Maruyama, Chem. Lett. (1991) 1225.
[8] R. Chiarelli, A. Rassat, P. Rey, J. Chem. Soc., Chem. Commun. (1992) 1081.
[9] P. Lahti (Ed.), Magnetic Properties of Organic Materials, Marcel Dekker, New York, 1999.
[10] D.B. Amabilino, J. Veciana, in: J.S. Miller, M. Drillon (Eds.), Magnetism: Molecules to Materials II. Molecule-Based Materials, Wiley–VCH, Weinheim, Germany, 2001, p. 1.

[11] Y.Y. Lim, R.S. Drago, Inorg. Chem. 11 (1972) 1334.
[12] P.F. Richardson, R.W. Kreilick, J. Am. Chem. Soc. 99 (1977) 8183.
[13] R. Briere, A. Rassat, P. Rey, J. Am. Chem. Soc. 100 (1978) 343.
[14] O.P. Anderson, T.C. Kuechler, Inorg. Chem. 19 (1980) 1417.
[15] M.H. Dickman, R.J. Doedens, Inorg. Chem. 20 (1981) 2677.
[16] L.C. Porter, M.H. Dickman, R.J. Doedens, Inorg. Chem. 22 (1983) 1962.
[17] A. Bencini, C. Benelli, D. Gatteschi, C. Zanchini, J. Am. Chem. Soc. 106 (1984) 5813–5818.
[18] M.H. Dickman, L.C. Porter, R.J. Doedens, Inorg. Chem. 25 (1986) 2595.
[19] L.C. Porter, M.H. Dickman, R.J. Doedens, Inorg. Chem. 25 (1986) 678.
[20] C.D. Smith, S.E. Bottle, P.C. Junk, K. Inoue, A.S. Markosyan, Synth. Met. 138 (2003) 501.
[21] E. Ressouche, J.X. Boucherle, B. Gillon, P. Rey, J. Schweizer, J. Am. Chem. Soc. 115 (1993) 3610.
[22] A. Zheludev, V. Barone, M. Bonnet, B. Delley, A. Grand, E. Ressouche, P. Rey, R. Subra, J. Schweizer, J. Am. Chem. Soc. 116 (1994) 2019.
[23] A. Caneschi, D. Gatteschi, J. Laugier, P. Rey, J. Am. Chem. Soc. 109 (1987) 2191.
[24] A. Caneschi, D. Gatteschi, P. Rey, R. Sessoli, Inorg. Chem. 27 (1988) 1756.
[25] A. Caneschi, D. Gatteschi, J.P. Renard, P. Rey, R. Sessoli, Inorg. Chem. 28 (1989) 3314.
[26] A. Caneschi, D. Gatteschi, J.P. Renard, P. Rey, R. Sessoli, Inorg. Chem. 28 (1989) 2940.
[27] A. Caneschi, F. Ferraro, D. Gatteschi, P. Rey, R. Sessoli, Inorg. Chem. 30 (1991) 3162.
[28] A. Caneschi, P. Chiesi, L. David, F. Ferraro, D. Gatteschi, R. Sessoli, Inorg. Chem. 32 (1993) 1445.
[29] A. Caneschi, D. Gatteschi, R. Sessoli, Inorg. Chem. 32 (1993).
[30] K. Inoue, T. Hayamizu, H. Iwamura, D. Hashizume, Y. Ohashi, J. Am. Chem. Soc. 118 (1996) 1803.
[31] H. Iwamura, K. Inoue, N. Koga, New J. Chem. 22 (1998) 201.
[32] F. Mathevet, D. Luneau, J. Am. Chem. Soc. 123 (2001) 7465.
[33] D. Luneau, G. Risoan, P. Rey, A. Grand, A. Caneschi, D. Gatteschi, J. Laugier, Inorg. Chem. 32 (1993) 5616.
[34] D. Luneau, P. Rey, J. Laugier, P. Fries, A. Caneschi, D. Gatteschi, R. Sessoli, J. Am. Chem. Soc. 113 (1991) 1245.
[35] P. Rey, D. Luneau, A. Cogne, In: NATO ASI Ser., Ser. E, vol. 198, 1991, p. 203.
[36] D. Luneau, P. Rey, J. Laugier, E. Belorizky, A. Cogne, Inorg. Chem. 31 (1992) 3578.
[37] C. Benelli, A. Caneschi, D. Gatteschi, L. Pardi, Inorg. Chem. 31 (1992) 741.
[38] H. Oshio, T. Watanabe, A. Ohto, T. Ito, U. Nagashima, Angew. Chem. Int. Ed. 33 (1994) 670.
[39] H. Oshio, T. Watanabe, A. Ohto, T. Ito, H. Masuda, Inorg. Chem. 35 (1996) 472.
[40] H. Oshio, T. Watanabe, A. Ohto, T. Ito, Inorg. Chem. 36 (1997) 1608.
[41] K. Fegy, N. Sanz, D. Luneau, E. Belorizky, P. Rey, Inorg. Chem. 37 (1998) 4518.
[42] H. Oshio, M. Yamamoto, T. Ito, J. Chem. Soc., Dalton Trans. (1999) 2641.
[43] C. Lescop, D. Luneau, P. Rey, G. Bussiere, C. Reber, Inorg. Chem. 41 (2002) 5566.
[44] A. Marvilliers, Y. Pei, J. Cano Boquera, K.E. Vostrikova, C. Paulsen, E. Rivière, J.-P. Audière, T. Mallah, J. Chem. Soc., Chem. Commun. (1999) 1951.
[45] K.E. Vostrikova, D. Luneau, W. Wernsdorfer, P. Rey, M. Verdaguer, J. Am. Chem. Soc. 122 (2000) 718.
[46] G. Francese, F.M. Romero, A. Neels, H. Stoeckli-Evans, S. Decurtins, Inorg. Chem. 39 (2000) 2087.
[47] K. Fegy, D. Luneau, T. Ohm, C. Paulsen, P. Rey, Angew. Chem. Int. Ed. 37 (1998) 1270.
[48] K. Fegy, D. Luneau, E. Belorizky, M. Novac, J.-L. Tholence, C. Paulsen, T. Ohm, P. Rey, Inorg. Chem. 37 (1998) 4524.
[49] K. Fegy, C. Lescop, D. Luneau, P. Rey, Mol. Cryst. Liq. Cryst. Sci. Technol., Sect. A: Mol. Cryst. Liq. Cryst. 334 (1999) 521.
[50] P. Rey, D. Luneau, NATO ASI Ser., Ser. C: Math. Phys. Sci. 518 (1999) 145.
[51] C. Lescop, D. Luneau, E. Belorizky, P. Fries, M. Guillot, P. Rey, Inorg. Chem. 38 (1999) 5472.
[52] C. Lescop, D. Luneau, P. Rey, MRS Symp. Proc. 598 (2000), BB3.49/1.
[53] C. Lescop, D. Luneau, G. Bussiere, M. Triest, C. Reber, Inorg. Chem. 39 (2000) 3740.
[54] C. Lescop, E. Belorizky, D. Luneau, P. Rey, Inorg. Chem. 41 (2002) 3375.
[55] D. Luneau, F.M. Romero, R. Ziessel, Inorg. Chem. 37 (1998) 5078.
[56] F.M. Romero, D. Luneau, R. Ziessel, J. Chem. Soc., Chem. Commun. (1998) 551.
[57] H. Oshio, T. Yaginuma, T. Ito, Inorg. Chem. 38 (1999) 2750.
[58] C. Stroh, E. Belorizky, P. Turek, H. Bolvin, R. Ziessel, Inorg. Chem. 42 (2003) 2938.
[59] R. Ziessel, Mol. Cryst. Liq. Cryst. 273 (1995) 101.
[60] Y. Pei, A. Lang, P. Bergerat, O. Kahn, M. Fettouhi, L. Ouahab, Inorg. Chem. 35 (1996) 193.
[61] J.-P. Sutter, M.L. Kahn, S. Golhen, L. Ouahab, O. Kahn, Chem. Eur. J. 4 (1998) 571.
[62] J.-P. Sutter, M.L. Kahn, O. Kahn, Adv. Mater. (Weinheim, Germany) 11 (1999) 863.
[63] M.L. Kahn, J.-P. Sutter, S. Golhen, P. Guionneau, L. Ouahab, O. Kahn, D. Chasseau, J. Am. Chem. Soc. 122 (2000) 3413.
[64] N. Yoshioka, M. Irisawa, N. Aizawa, T. Aoki, H. Inoue, S. Ohba, Mol. Cryst. Liq. Cryst. 286 (1996) 487.
[65] N. Yoshioka, M. Irasawa, Y. Mochizuki, T. Kato, H. Inoue, S. Ohba, Chem. Lett. (1997) 251.
[66] N. Yoshioka, M. Irasawa, M. Abe, T. Aoki, N. Aizawa, H. Inoue, S. Ohba, Mol. Cryst. Liq. Cryst. 306 (1997) 397.
[67] N. Yoshioka, M. Irisawa, Y. Mochizuki, T. Aoki, H. Inoue, Mol. Cryst. Liq. Cryst. 306 (1997) 403.
[68] H. Tamaki, Z.J. Zhong, N. Matsumoto, S. Kida, M. Koikawa, N. Achiwa, Y. Hashimoto, H. Okawa, J. Am. Chem. Soc. 114 (1992) 6974.
[69] O. Kahn, in: E. Coronado, P. Delhaès, D. Gatteschi, J.S. Miller (Eds.), Molecular Magnetism: From Molecular Assemblies to the Devices, vol. 321, Kluwer Academic Publishers, Dordrech, 1996, p. 243.
[70] M. Pilkington, S. Decurtins, in: J.S. Miller, M. Drillon (Eds.), Magnetism: Molecules to Materials II. Molecule-Based Materials, Wiley–VCH, Weinheim, Germany, 2001, p. 339.
[71] E.F. Ullman, J.H. Osiecky, D.G.B. Boocock, R. Darcy, J. Am. Chem. Soc. 94 (1972) 7049.
[72] E.F. Ullman, L. Call, J.H. Osiecky, J. Org. Chem. 35 (1970) 3623.
[73] C. Hirel, K.E. Vostrikova, J. Pécaut, V.I. Ovcharenko, P. Rey, Chem. Eur. J. 7 (2001) 2007.
[74] Typically a solution of nitronyl nitroxide (1 g) in 100 mL of CH_2Cl_2 is cooled on an ice bath and mixed with a solution of $NaNO_2$ in large excess (1 g) in 100 mL of distilled water then a HCl solution (0.2 M) is dropped on the mixture. The imino-nitroxyde is formed at the expense of the nitronyl-nitroxide. The progress of the reaction is followed by TLC on silica gel and addition of HCl is stopped when the reaction seem no more to evolve. The imino nitroxide is purified by extraction from the aqueous phase followed by column chromatography on silica gel.
[75] O. Kahn, Molecular Magnetism, VCH Publishers, New York, 1993.
[76] J. Seiden, J. Phys. Lett. 44 (1987) 947.

[77] M.A. Martinez-Lorente, J.-P. Tuchagues, V. Pétrouléas, J.-M. Savariault, R. Poinsot, M. Drillon, Inorg. Chem. 30 (1991) 3589.
[78] P. Day, J. Chem. Soc., Dalton. Trans. (1997) 701.
[79] S. Decurtins, H.W. Schmalle, P. Schneuwly, H.R. Oswald, Inorg. Chem. 32 (1993) 1888.
[80] C. Lescop, G. Bussiere, R. Beaulac, H. Bélisle, E. Belorizky, P. Rey, C. Reber, D. Luneau, J. Phys. Chem. Sol. 65 (2004) 773.
[81] T. Tsukuda, T. Suzuki, S. Kaizaki, J. Chem. Soc., Dalton Trans. (2002) 1721.
[82] C. Benelli, A. Caneschi, D. Gatteschi, J. Laugier, P. Rey, Angew. Chem., Int. Ed. 26 (1987) 913.
[83] C. Benelli, A. Caneschi, D. Gatteschi, L. Pardi, P. Rey, Inorg. Chem. 29 (1990) 4223.
[84] A. Caneschi, A. Dei, D. Gatteschi, L. Sorace, K.E. Vostrikova, Angew. Chem., Int. Ed. 39 (2000) 246.
[85] C. Benelli, D. Gatteschi, Chem. Rev. 102 (2002) 2369.
[86] M. Andruh, I. Ramade, E. Godjovi, O. Guillou, O. Kahn, J.-C. Trombe, J. Am. Chem. Soc. 115 (1993) 1822.
[87] G. Bussière, R. Beaulac, H. Bélisle, C. Lescop, D. Luneau, P. Rey, C. Reber, Top. Curr. Chem. 241 (2004) 97.
[88] M. Ogita, Y. Yamamoto, T. Suzuki, S. Kaizaki, Eur. J. Inorg. Chem. (2002) 886.
[89] T. Yoshida, K. Kanamori, S. Takamizawa, W. Mori, S. Kaizaki, Chem. Lett. (1997) 603.
[90] T. Yoshida, T. Suzuki, K. Kanamori, S. Kaizaki, Inorg. Chem. 38 (1999) 1059.
[91] P.J. McCarthy, H.U. Güdel, Coord. Chem. Rev. 88 (1988) 69.
[92] J.-P. Costes, F. Dahan, A. Dupuis, J.-P. Laurent, Inorg. Chem. 39 (2000) 169.